Title

Drosophila Histone Demethylase KDM4A Has Enzymatic and Non-enzymatic Roles in Controlling Heterochromatin Integrity

Journal

Developmental Cell, 42(2)

ISSN

1534-5807

Authors

Colmenares, Serafin U
Swenson, Joel M
Langley, Sasha A
et al.

Publication Date

2017-07-01

DOI

10.1016/j.devcel.2017.06.014

Peer reviewed

Article

Developmental Cell

Drosophila Histone Demethylase KDM4A Has Enzymatic and Non-enzymatic Roles in Controlling Heterochromatin Integrity

Graphical Abstract

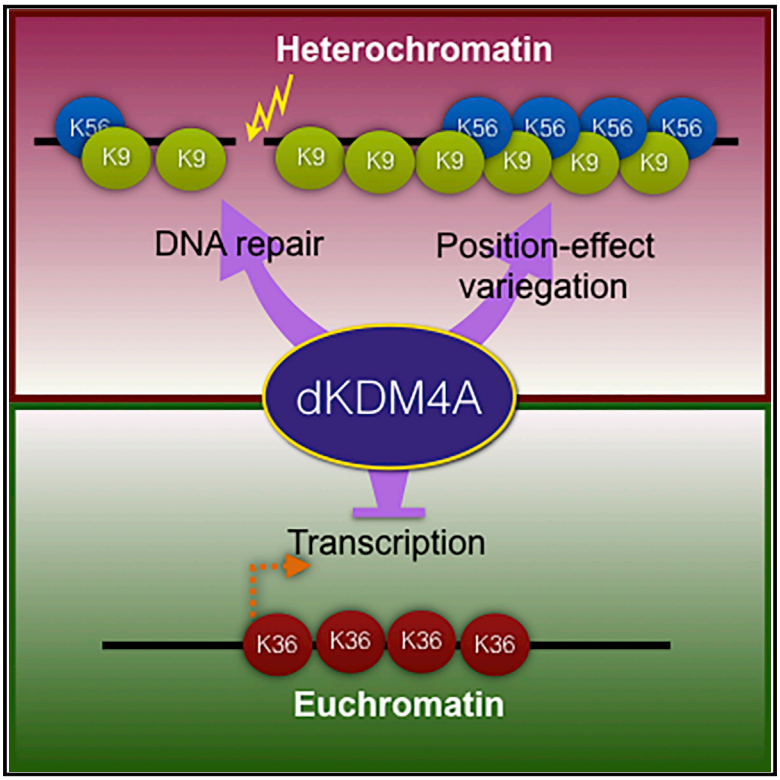

Authors

Serafin U. Colmenares, Joel M. Swenson, Sasha A. Langley, Cameron Kennedy, Sylvain V. Costes, Gary H. Karpen

Correspondence

sucolmenares@lbl.gov

In Brief

Colmenares et al. discover that *Drosophila* KDM4A, previously characterized as a euchromatic histone H3K36 demethylase and transcriptional regulator, is recruited to heterochromatin to contribute non-enzymatically to position-effect variegation, a hallmark of heterochromatin integrity. Conversely, dKDM4A catalytic activity is vital to heterochromatin DNA repair and is associated with demethylation of heterochromatic H3K56me3.

Highlights

- dKDM4A is enriched in heterochromatin in an HP1a-dependent manner
- dKDM4A has distinct functions between euchromatin and heterochromatin
- dKDM4A plays a demethylase-independent role in position-effect variegation
- dKDM4A demethylates heterochromatic H3K56me3 after DNA damage

Colmenares et al., 2017, Developmental Cell *42*, 156–169
July 24, 2017
http://dx.doi.org/10.1016/j.devcel.2017.06.014

CellPress

CellPress

Developmental Cell
Article

Drosophila Histone Demethylase KDM4A Has Enzymatic and Non-enzymatic Roles in Controlling Heterochromatin Integrity

Serafin U. Colmenares,[1,3,*] Joel M. Swenson,[1,2] Sasha A. Langley,[1] Cameron Kennedy,[1] Sylvain V. Costes,[1] and Gary H. Karpen[1,2]

[1]Biological Systems and Engineering, Lawrence Berkeley National Laboratory, Berkeley, CA 94720, USA
[2]Department of Molecular and Cellular Biology, University of California, Berkeley, CA 94720, USA
[3]Lead Contact
*Correspondence: sucolmenares@lbl.gov
http://dx.doi.org/10.1016/j.devcel.2017.06.014

SUMMARY

Eukaryotic genomes are broadly divided between gene-rich euchromatin and the highly repetitive heterochromatin domain, which is enriched for proteins critical for genome stability and transcriptional silencing. This study shows that *Drosophila* KDM4A (dKDM4A), previously characterized as a euchromatic histone H3 K36 demethylase and transcriptional regulator, predominantly localizes to heterochromatin and regulates heterochromatin position-effect variegation (PEV), organization of repetitive DNAs, and DNA repair. We demonstrate that dKDM4A demethylase activity is dispensable for PEV. In contrast, dKDM4A enzymatic activity is required to relocate heterochromatic double-strand breaks outside the domain, as well as for organismal survival when DNA repair is compromised. Finally, DNA damage triggers dKDM4A-dependent changes in the levels of H3K56me3, suggesting that dKDM4A demethylates this heterochromatic mark to facilitate repair. We conclude that dKDM4A, in addition to its previously characterized role in euchromatin, utilizes both enzymatic and structural mechanisms to regulate heterochromatin organization and functions.

INTRODUCTION

Heterochromatin (HC) comprises 20% and 30% of human and *Drosophila* genomes (Lander et al., 2001; Hoskins et al., 2007), respectively, and remains condensed throughout the cell cycle (Heitz, 1928). HC composition is distinct from euchromatin (EC), with its low gene count and high enrichment for repetitive sequences, di- and tri-methylated histone H3 K9 (H3K9me2 and 3), and Heterochromatin Protein 1a (HP1a) (Eissenberg and Elgin, 2000). HC is concentrated at pericentromeric and telomeric regions (Karpen and Allshire, 1997), where it plays important roles in genome stability. Disruption of HC structure impairs chromosome segregation (Kellum and Alberts, 1995), replication timing (Barigozzi et al., 1966), transposon silencing (Rangan et al., 2011), gene expression (Weiler and Wakimoto, 1995; Piacentini and Pimpinelli, 2010), and DNA repair (Peng and Karpen, 2009). However, the mechanisms by which HC components mediate these diverse processes remain poorly understood.

Central to HC structure is the enrichment for H3K9me2 and me3, primarily catalyzed by the histone methyltransferase (HMTase) Su(var)3–9 (Schotta et al., 2002). These methyl marks form the epigenetic basis for HC maintenance by providing binding sites for HP1a (Bannister et al., 2001). HP1a, in turn, recruits other proteins that mediate the many chromosomal and nuclear functions of HC (Alekseyenko et al., 2014; Ryu et al., 2014; Swenson et al., 2016). Loss of Su(var)3–9, HP1a, or other HC proteins leads to defects in HC function (Eissenberg et al., 1990; Tschiersch et al., 1994), which can be observed as changes in the silencing of genes inserted into or near HC (position-effect variegation or PEV) (Grigliatti, 1991). Reporter genes placed in proximity to HC undergo stochastic silencing due to variable spreading of HC proteins, and become derepressed or further silenced upon disruption or augmentation of HC components, respectively (Weiler and Wakimoto, 1995). Genetic screens for PEV modifiers have identified ~150 genes that regulate HC function (Schotta et al., 2003), but the identities of the majority of these genes and their molecular roles in HC structure and function are unknown.

Accumulating evidence shows that HC components are critical for genome integrity and play important roles in DNA repair (Dinant and Luijsterburg, 2009; Cann and Dellaire, 2011). Loss of the Su(var)3–9 HMTase leads to chromosome segregation defects, repetitive DNA instability, and accumulation of DNA repair protein foci, including phosphorylated H2A variant (γH2Av) (Peng and Karpen, 2007). Su(var)3–9, HP1a, and the Smc5/6 complex also facilitate repair of heterochromatic double-strand breaks (DSBs) by the homologous recombination (HR) pathway, which utilizes a distinct and dynamic spatiotemporal regulatory mechanism (Chiolo et al., 2011). Early steps in HR repair, such as end resection, occur within minutes after DNA damage inside the HC domain. However, Rad51 recruitment, which is required to complete HR repair (Eskeland et al., 2007), only occurs after DSBs are relocalized outside the HC domain and associate with the nuclear periphery (Ryu et al., 2015). This spatial partitioning of HR events enables the separation of repeats with DSBs from the rest of the HC, which likely

reduces the probability of reciprocal exchange that results in genome instability (e.g., translocations that form acentric and dicentric chromosomes), and promotes less harmful HR repair from homologs or sister chromatids (Chiolo et al., 2011).

The *Drosophila* KDM4A (dKDM4A) protein belongs to the jumonji family of Fe(II)- and α-ketoglutarate-dependent lysine demethylases (Whetstine et al., 2006). Members of this family play vital roles in epigenetic mechanisms that govern gene expression and development (Nottke et al., 2009; Lorbeck et al., 2010), regulate DNA repair and genome stability (Mallette et al., 2012; Kupershmit et al., 2014; Awwad and Ayoub, 2015), and are misregulated in many types of cancers (Black et al., 2013; Guerra-Calderas et al., 2015). Despite its name, the closest dKDM4A mammalian homolog is KDM4D, since both contain the JmjN and JmjC domains responsible for enzymatic activity, and lack the PHD and Tudor domains found in human KDM4A (Lloret-Llinares et al., 2008). dKDM4A catalyzes the demethylation of H3K36me3 and H3K36me2 *in vitro* and *in vivo* (Lin et al., 2008; Crona et al., 2013), suggesting a transcriptional role, as these modifications are hallmarks of active gene bodies (Xiao et al., 2003). Consequently, recent studies have focused on how dKDM4A regulates gene activity in EC (Lin et al., 2008) (Crona et al., 2013).

dKDM4A homologs, as well as the closely related fly homolog KDM4B, have also been reported to demethylate H3K9me3. However, an *in vitro* study (Lin et al., 2008) concluded that dKDM4A lacks the H3 K9 demethylase activity associated with mammalian family members and dKDM4B (Klose et al., 2006; Lin et al., 2008); thus dKDM4A-dependent changes in H3K9me3 levels observed *in vivo* in flies are likely indirect or require additional cofactors (Lloret-Llinares et al., 2008; Tsurumi et al., 2013). KDM4A homologs have also been shown to demethylate other HC-associated modifications, including H1.4K26me3 (Trojer et al., 2009) and H3K56me3 (Jack et al., 2013). However, *Drosophila* H1 lacks the lysine methylated in other species, and H3K56me3 has not been tested as a dKDM4A substrate in flies. Interestingly, dKDM4A contains a PxVxL motif that mediates its interaction with HP1a (Lin et al., 2008). Surprisingly, despite these links to HC, a potential role for dKDM4A in regulating HC structure or function has not been reported.

This study demonstrates that *Drosophila* KDM4A is highly enriched in HC and is required for normal HC structure and function, including repair of DNA damage. We show that dKDM4A affects transcription of some EC genes, but find limited evidence for transcriptional regulation of heterochromatic genes and transposons. Instead, we show that dKDM4A is required for the spatial organization of repetitive elements, PEV, and the mobilization and repair of HC DSBs. We further determine that dKDM4A contributes a structural, non-catalytic role in maintenance of HC integrity, as assayed by PEV. In contrast, we show that dKDM4A catalytic activity is important for relocalization of DSBs outside the HC domain and for organismal survival of DNA repair mutants. Finally, we find that DNA damage triggers dKDM4A-dependent changes in the levels of heterochromatic H3K56me3. Altogether, we conclude that dKDM4A is an HC component vital to the stability and organization of repetitive DNA and HC-mediated gene silencing, through a combination of structural and enzymatic functions.

RESULTS

dKDM4A Is Highly Enriched in HC throughout the Cell Cycle

Previous studies reported that overexpressed dKDM4A localizes to EC in polytene tissues, and emphasized its role in H3K36 demethylation at active EC genes (Lin et al., 2008; Lloret-Llinares et al., 2008; Tsurumi et al., 2013). Based on its physical interactions with HP1a, we investigated the potential involvement of dKDM4A in HC structure and function. We first tested the nuclear localization of dKDM4A using immunofluorescence (IF) of the native protein. However, a lab-generated antibody to dKDM4A that detects the protein in western blots failed to produce any nuclear signal after IF (data not shown). We therefore analyzed the live nuclear localization of dKDM4A in Schneider-2 (S2) cells stably expressing low levels of fluorescently tagged dKDM4A and HP1a. In flies, pericentromeric regions from chromosomes X, 2, and 3, and all of chromosomes Y and 4, coalesce during interphase into a HP1a-enriched HC domain spatially separated from EC and positioned adjacent to the nucleolus (Elgin and Reuter, 2013). Our study showed that the vast majority of dKDM4A co-localized extensively with HP1a (Figure 1A) and is therefore highly enriched in HC. Similar results were obtained with mCherry-dKDM4A and GFP-HP1a stably co-expressed in early embryonic Kc and neuronal BG3 cell lines (Figure S1A), showing that dKDM4A is consistently enriched in HC in various *Drosophila* cell types. Moreover, dKDM4A localization is not affected by expression levels; transient co-transfection of GFP-dKDM4A and mCherry-HP1a revealed that dKDM4A co-localized with HP1a even at the lowest levels detectable by live imaging.

dKDM4A co-localization with HP1a closely follows the dynamic distribution of HP1a during the cell cycle. HP1a is released from chromosomes in early mitosis and reassembles into a cohesive domain in G_1 (Kellum and Alberts, 1995). In time-lapse movies, GFP-dKDM4A and mCherry-HP1a extensively co-localize throughout interphase and simultaneously become dispersed in early mitosis (Figure 1B). HC enrichment of both proteins initiates in anaphase/telophase, and is fully restored by the start of G_1. dKDM4A recruitment to HC after mitosis is delayed relative to HP1a enrichment, suggesting dependence of dKDM4A on HP1a for HC localization (see below). Both proteins also remain enriched in HC during S phase (identified by mCherry-tagged PCNA, Figure 1C). As HC DNA replicates during late S phase, PCNA foci form on or around HP1a- and dKDM4A-enriched regions. We conclude that dKDM4A retains its HC localization and enrichment throughout the dynamic changes that occur during the cell cycle.

dKDM4A Localization to HC Requires Su(var)3–9 and HP1a

RNAi depletion was used to evaluate the epistasis relationships between HP1a, Su(var)3–9, and dKDM4A. RNAi of dKDM4A or brown control (bw) had no effect on HP1a subnuclear enrichment or protein levels in S2 cells, demonstrating that HP1a localization to HC does not depend on dKDM4A (Figures 1D and 1E). In contrast, HP1a or Su(var)3–9 RNAi resulted in loss of dKDM4A HC enrichment and an increase in diffuse pan-nuclear signals (Figure 1D). Small HP1a foci persist after Su(var)3–9 RNAi, likely due to (1) the presence of two minor H3K9 HMTases (*G9a*

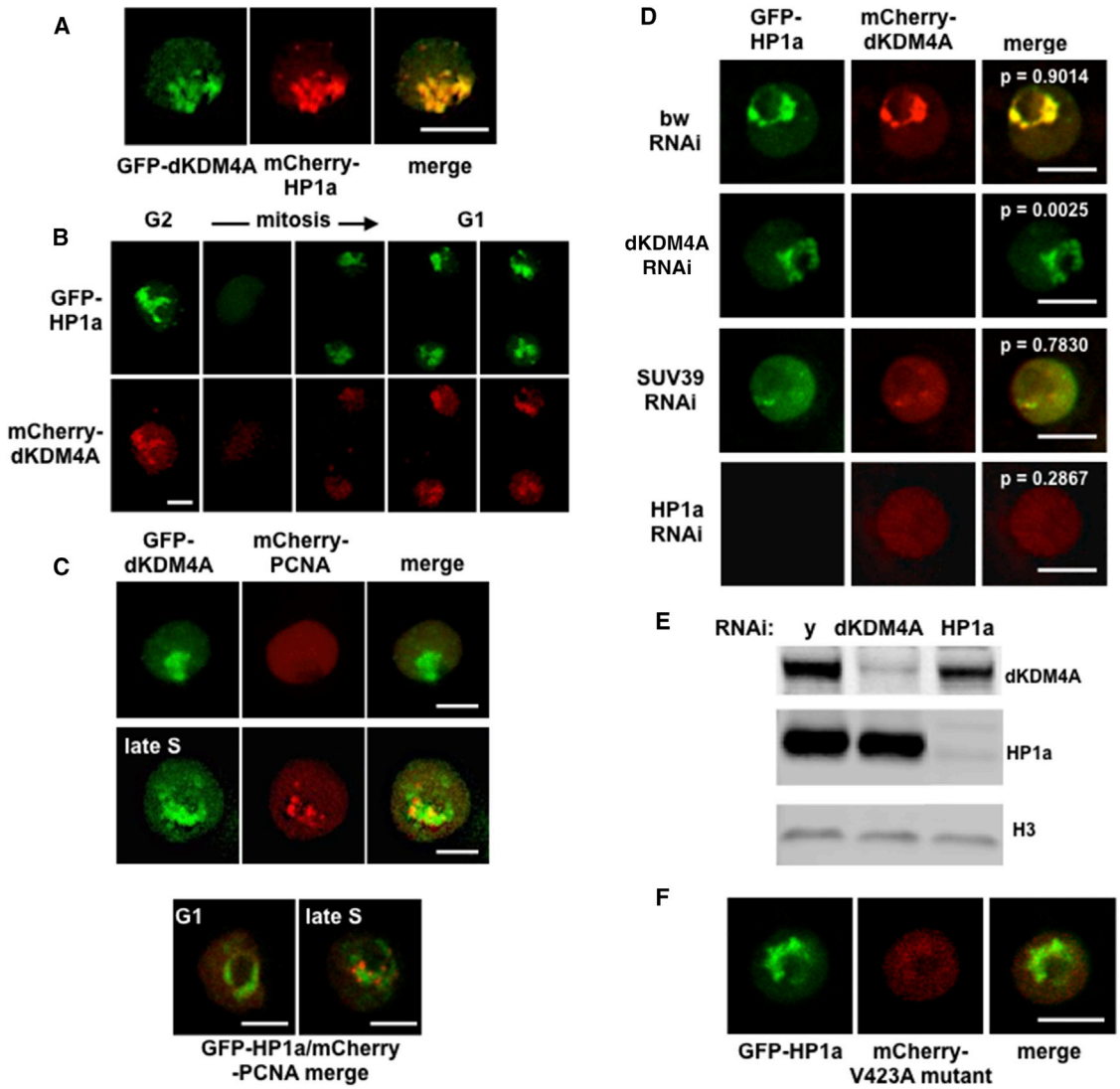

Figure 1. dKDM4A Is Enriched in HC

(A) Live imaging of S2 cells stably expressing GFP-tagged dKDM4A and mCherry-tagged HP1a.

(B) Time-lapse imaging of BG3 cells transiently expressing GFP-tagged HP1a and mCherry-tagged dKDM4A from G2 to G1. Dispersion of HP1a marks progression of cells through mitosis.

(C) Time-lapse imaging of BG3 cells transiently expressing GFP-tagged dKDM4A or HP1a, and mCherry-tagged PCNA shows continued HC enrichment of dKDM4A (above) and HP1a (below) during late S phase, as marked by PCNA replication foci in HC.

(D) Live imaging of Kc cells stably expressing GFP-HP1a and mCherry-dKDM4A after 5-day RNAi of bw (control), dKDM4A, Su(var)3–9, or HP1a. Pearson coefficient of correlation (p) is shown in merged images of bw (n = 25), dKDM4A (n = 22), Su(var)3–9 (n = 27), and HP1a RNAi (n = 23).

(E) Western blot analysis of S2 cell extracts after 5-day RNAi of y (control), dKDM4A, or HP1a.

(F) Live imaging of S2 cells transiently expressing GFP-tagged HP1a and mCherry-tagged dKDM4A mutated for the PxVxL motif required for HP1a binding. Scale bars, 5 μm. See also Figure S1.

and *eggless*) responsible for methylation of specific domains (Seum et al., 2007) and/or (2) HP1a localization to telomeres, which occurs independently of H3K9 methylation (Fanti et al., 1998). Regardless, we observe that Su(var)3–9-independent HP1a foci are also enriched for dKDM4A. Finally, dKDM4A mutated at the PxVxL motif (V423A) required for binding the HP1a chromoshadow domain (CSD) (Lin et al., 2008) showed lack of enrichment in HP1a-marked HC (Figure 1F). We conclude that dKDM4A is recruited to HC by Su(var)3–9 and HP1a through its PxVxL domain, but is not required for HP1a enrichment in HC.

To further characterize the dKDM4A association with HC, we used fluorescence recovery after photobleaching (FRAP) to compare the dynamics of dKDM4A within and outside HC. Previously, HP1a FRAP displayed both highly dynamic and stable components (Cheutin et al., 2003). Our FRAP results show that the HC dKDM4A population is more dynamic than HP1a (Figure S1B), suggesting that dKDM4A-HP1a interactions are less stable than HP1a interactions with the HC domain. The EC dKDM4A population is even more dynamic than the HC population and closely matches the behavior of a dKDM4A PxVxL

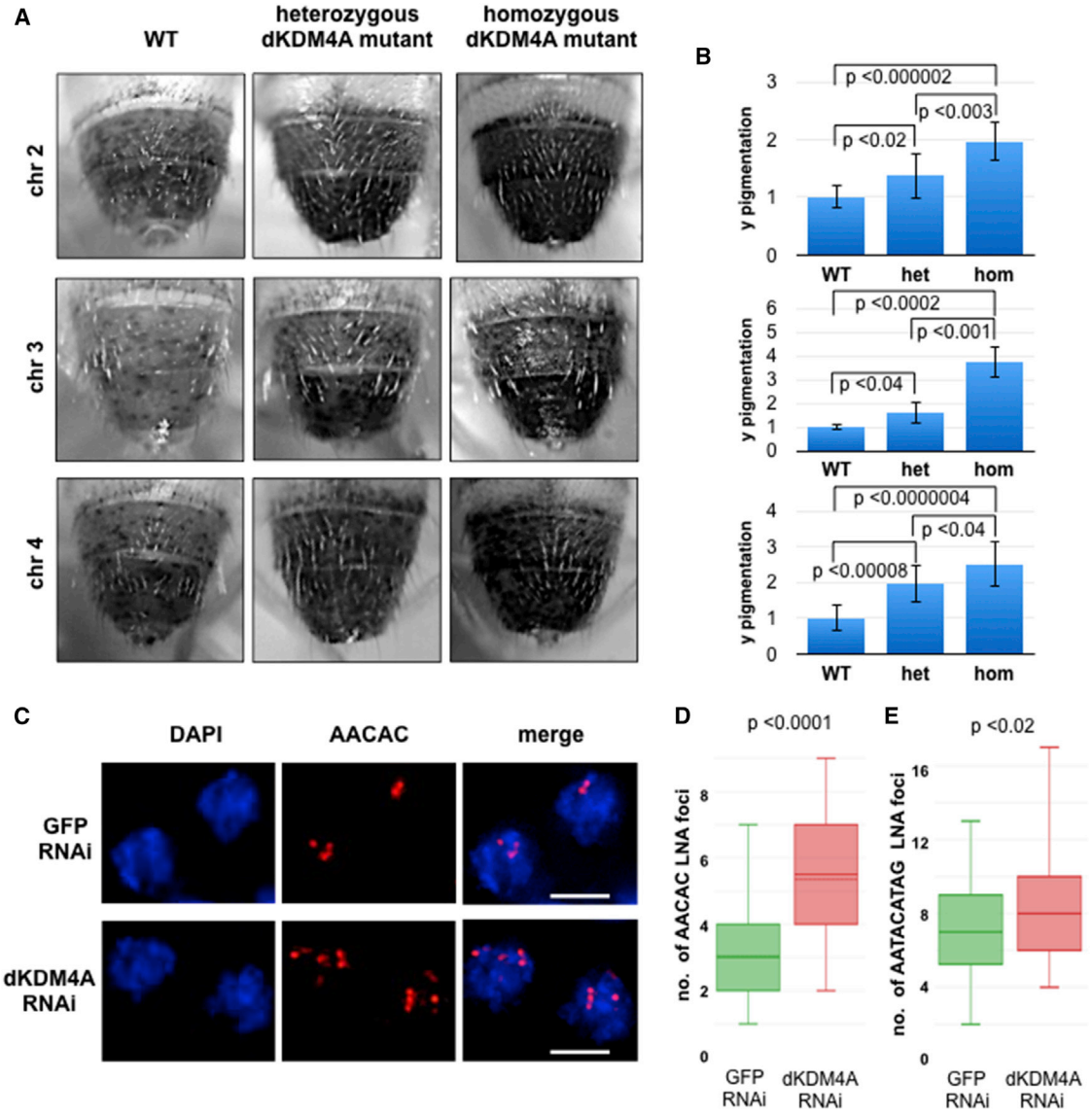

Figure 2. Position-Effect Variegation Is Dependent on dKDM4A Levels

(A) Representative images of wild-type (WT) and mutant dKDM4A fly abdomens exhibiting silencing effects on a y^+ reporter gene inserted in different HC regions of chromosomes 2, 3, and 4. Images represent the median of at least 10 individuals.

(B) Fiji-based quantitation of pigmentation on the last two abdominal segments is shown for wild-type and dKDM4A mutant flies for each reporter gene strain. Error bars representing SD and p values are shown.

(C) Representative FISH images of S2 cells showing AACAC tandem repeats after GFP (control) or dKDM4A RNAi. Scale bars, 5 μm. Number of AACAC repeat foci is quantitated in (D), and a similar experiment in Kc cells using LNA probes for AATAACATAG is quantitated in (E). Error bars representing SD and p values are shown. See also Figure S2.

mutant that cannot bind HP1a in HC. This suggests that HP1a binding stabilizes dKDM4A in HC. In contrast, HP1a dynamics in HC are not markedly affected by loss of dKDM4A (Figure S1C), consistent with dKDM4A acting downstream of HP1a. Overall, based on strong dKDM4A enrichment in HC, and its recruitment and stabilization by HP1a binding, we conclude that dKDM4A is a structural component of HC.

dKDM4A Is Required for HC-Mediated Gene Silencing

To determine whether dKDM4A is required for HC functions, we tested the impact of altered dKDM4A dosage on HC-mediated gene silencing (PEV). The *yellow*$^+$ (y^+) reporter gene, when inserted into HC, exhibits stochastic expression represented by dots of dark pigment on the dorsal abdomen of adult flies (Figure 2A). Loss of Su(var)3–9, HP1a, or other known HC components results in suppression of PEV, which can be visualized as increased pigmentation. We observe that a dKDM4A mutation that completely abolishes dKDM4A protein (Figure S2) also derepresses heterochromatic reporter genes in a dose-dependent fashion. Flies heterozygous for dKDM4A display significantly increased abdominal pigmentation compared with wild-type flies; flies completely lacking a functional dKDM4A

resulted in even higher pigmentation levels (Figures 2A and 2B). Similar suppression of PEV in the absence of dKDM4A was observed for y^+ reporter genes inserted in the pericentric HC of chromosomes 2 (top), 3 (middle), and 4 (bottom). Therefore, we conclude that wild-type dKDM4A is required for gene silencing in different HC regions, and, like HP1a or Su(var)3–9 mutants, a dKDM4A loss-of-function mutation acts as a dominant suppressor of variegation.

dKDM4A Is Required for Repeat Organization in HC

dKDM4A effects on PEV indicate that HC is perturbed in mutants, yet we observed no change in HP1a localization and dynamics after dKDM4A RNAi in tissue culture cells. We therefore determined whether dKDM4A affects higher-order HC architecture, specifically the organization of satellite DNA in HC, using tandem repeat probes and fluorescence in situ hybridization (FISH). We analyzed the distribution of two tandem repeats (AACAC of chromosome 2 and AATAACATAG of chromosomes 2 and 3) in S2 and Kc cells depleted for dKDM4A, yellow (y), or GFP. We observed that loss of dKDM4A increased the average number of repeat foci per nucleus (Figures 2C–2E) and the average distance between the most distal foci in a nucleus (Figure S2B), and decreased the size and intensity of satellite foci (Figure S2C). We also detected an increased number of AACAC, AATAACATAG, and dodeca (chromosome 3) foci in whole-mount, polytene cells from dKDM4A mutant flies, validating a role for dKDM4A satellite architecture in the animal (Figures S2D and S2E). We conclude that although dKDM4A acts downstream of HP1a, and is not required for gross localization of HP1a to HC, it is still required to establish or maintain the 3D organization of repeated sequences in HC.

dKDM4A Does Not Significantly Affect Transcription in HC

HC contains fewer genes and lower levels of active transcription marks compared with EC, but nevertheless contains active genes and transposable elements (Riddle et al., 2011). Loss of dKDM4A alters gene expression in flies (Crona et al., 2013) and increases H3K36me3 levels at several HC genes (Lin et al., 2012). However, these studies did not include the majority of HC genes, or any transposable elements or tandem repeats enriched in HC.

To study the broad effects of dKDM4A on HC transcription, we compared S2 cells depleted for dKDM4A, HP1a, or GFP (control). A 5-day RNAi of dKDM4A in S2 cells resulted in near-complete absence of dKDM4A protein and a nearly 50% increase in bulk H3K36me3 levels, in comparison with GFP RNAi (Figure 3A). Therefore, if dKDM4A regulates HC function through demethylation of H3K36me3, dKDM4A loss should result in increased HC gene and repeat transcript levels.

The RNA-sequencing results show that dKDM4A regulates a smaller fraction of *Drosophila* genes than HP1a. Out of 14,869 genes analyzed, only 66 are upregulated after dKDM4A depletion, compared with 304 genes upregulated after HP1a RNAi (Figure 3B; Tables S1 and S2). Interestingly, 35 of these dKDM4A-regulated genes are also activated by loss of HP1a, indicating that they are co-repressed by these HC factors. In addition, 22 genes are downregulated after dKDM4A RNAi, compared with 183 genes for HP1a RNAi, of which six are co-regulated by dKDM4A and HP1a. dKDM4A gene targets are widely distributed throughout the genome, but include only two HC genes, suggesting that dKDM4A regulates transcription of a small number of mostly EC genes. In contrast, HP1a regulates 50 HC genes (Figures 3B and S3A). Comparison of dKDM4A RNAi effects on transcription with previously published data from a dKDM4A mutant fly (Crona et al., 2013) shows little overlap (4 out of 99 dKDM4A-affected genes), suggesting that gene regulation by dKDM4A may differ between tissue culture and flies.

In addition, there was no significant activation of transposable element or repeat transcription after dKDM4A RNAi, in contrast to the upregulation of 34 transposons and the 1.688 satellite repeat after HP1a RNAi (Figure 3C). Whether or not dKDM4A exerts transcriptional effects on non-polyadenylated HC transcripts remains to be determined. Notably, two transposable elements primarily found near telomeres (TAHRE and Het-A) were downregulated after dKDM4A or HP1A RNAi (Figure 3D), and thus require dKDM4A and HP1a for normal transcription levels. The possibility that dKDM4A is involved in telomere structure or function, as observed for HP1a (Savitsky et al., 2002), is consistent with the observed co-localization of dKDM4A-enriched foci with a telomere-capping protein, HOAP (Figure S3B), and the co-localization of dKDM4A with Su(var)3–9-independent HP1a foci (Figure 1D). Regardless, unlike HP1a, dKDM4A enrichment at pericentric HC is not connected with regulation of most transposon transcriptional activity, suggesting other functions of dKDM4A in HC. Overall, we conclude that dKDM4A plays a relatively minor role in regulating the transcription of HC genes and transposons.

dKDM4A Loss Alters H3K9me3 but Not H3K36me3 Levels in HC

HC contains overall lower levels of H3K36me3 compared with EC (Riddle et al., 2011), which in part may be due to the enrichment of dKDM4A in HC. To determine whether the dKDM4A-dependent increases in H3K36me3 levels (Figure 3A) occurs in HC or EC, we performed IF in Kc cells after dKDM4A RNAi. In control cells, we observed that HP1a- or H3K9me2-enriched regions contain very low levels of H3K36me3, whereas EC regions with low HP1a or H3K9me2 staining exhibited high H3K36me3 enrichment (Figure 4A). However, low H3K36me3 levels persist in dKDM4A-depleted HC, while dKDM4A-depleted EC regions exhibit brighter H3K36me3 intensities compared with control cells (Figures 4A and 4B). These results suggest that dKDM4A-mediated demethylation is not responsible for the overall low levels of H3K36me3 in HC, but does affect the levels of this modification in EC.

Although dKDM4A does not demethylate H3K9me3 *in vitro* (Lin et al., 2008), other studies suggest that dKDM4A reduces H3K9me3 levels *in vivo* (Lloret-Llinares et al., 2008; Tsurumi et al., 2013), which could account for dKDM4A effects on HC functions. To test this hypothesis and generate a higher-resolution map of both H3K9me3 and H3K36me3 enrichments across the genome, we performed chromatin immunoprecipitation sequencing (ChIP-seq) analysis of S2 cells after dKDM4A or GFP (control) RNAi. Using antibodies previously validated by modENCODE (Egelhofer et al., 2011), ChIP-seq results showed significantly higher enrichment levels of both H3K36me3 and

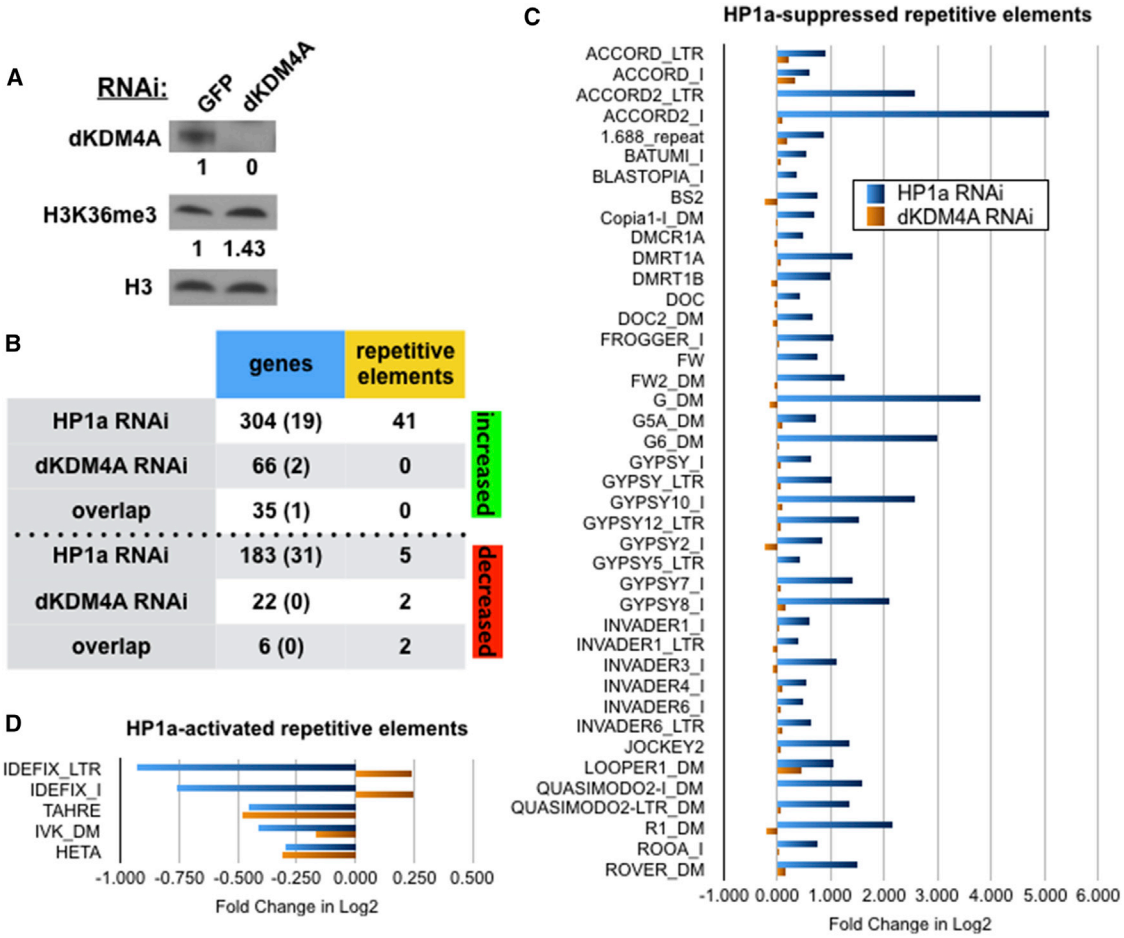

Figure 3. dKDM4A Does Not Significantly Contribute to Transcriptional Regulation of HC Elements

(A) Representative western blot analysis of dKDM4A and H3K36me3 levels after 5 days' RNAi depletion of dKDM4A, compared with GFP RNAi (control). Fiji-based quantitation of dKDM4A and H3K36me3 levels after normalization to GFP RNAi levels and the H3 loading control is shown below.

(B) Number of genes and repetitive elements showing a significant change in RNA levels after 5-day dKDM4A or HP1a RNAi in S2 cells, compared with a GFP RNAi control; $p < 0.05$. Number of HC genes affected by either dKDM4A or HP1a RNAi is shown in parentheses. "Overlap" row indicates the number of genes and repetitive elements co-regulated by dKDM4A and HP1a.

(C) Repetitive-element transcript levels increased by HP1a RNAi (blue) over GFP RNAi are contrasted with their levels after dKDM4A RNAi (orange).

(D) HP1a RNAi-induced decreases in repetitive-element transcript levels are contrasted with dKDM4A RNAi effects.

See also Figure S3; Tables S1 and S2.

H3K9me3 peaks in EC after dKDM4A knockdown (Figure 4C). However, dKDM4A RNAi had no effect on the enrichment of H3K36me3 peaks in HC, consistent with the IF results, but did display a moderate increase in the enrichment levels of H3K9me3 peaks (Figure 4D).

Standard ChIP-seq analyses focus on uniquely mapping sequences, which represent only a minor part of HC. Therefore, we also analyzed the effects of dKDM4A RNAi on H3K36me3 and H3K9me3 enrichments in repetitive DNA. We observed that satellite sequences, histone genes, and ribosomal DNA were not enriched for H3K36me3 in controls (Figure 4E). Furthermore, although many transposons (e.g., those enriched at telomeres) contained high levels of H3K36me3 in control samples, enrichments at these transposons or any other repetitive DNA tested did not significantly change after dKDM4A RNAi. Thus, we conclude that dKDM4A effects on HC structure (e.g., satellite organization) or function (e.g., PEV) are independent of its H3K36me3 demethylase activity.

In contrast, H3K9me3 enrichment at repetitive domains (two satellite sequences and a transposon) exhibited either significant loss or gain of H3K9me3 enrichment after dKDM4A depletion, and the entire population of transposons showed generally higher H3K9me3 enrichment (Figure 4F, trendline). We conclude that dKDM4A affects H3K9me3 levels in different HC domains. Although this suggests that dKDM4A could influence PEV directly through H3K9me3 demethylation, this is inconsistent with (1) the lack of *in vitro* H3K9 demethylation activity for dKDM4A (Lin et al., 2008), (2) the presence of both gains and losses of H3K9 methylation, and (3) catalytic activity not being required for suppressing PEV (see next section). Thus, changes to H3K9me3 levels are more likely to result from indirect effects arising from HC structural disorganization

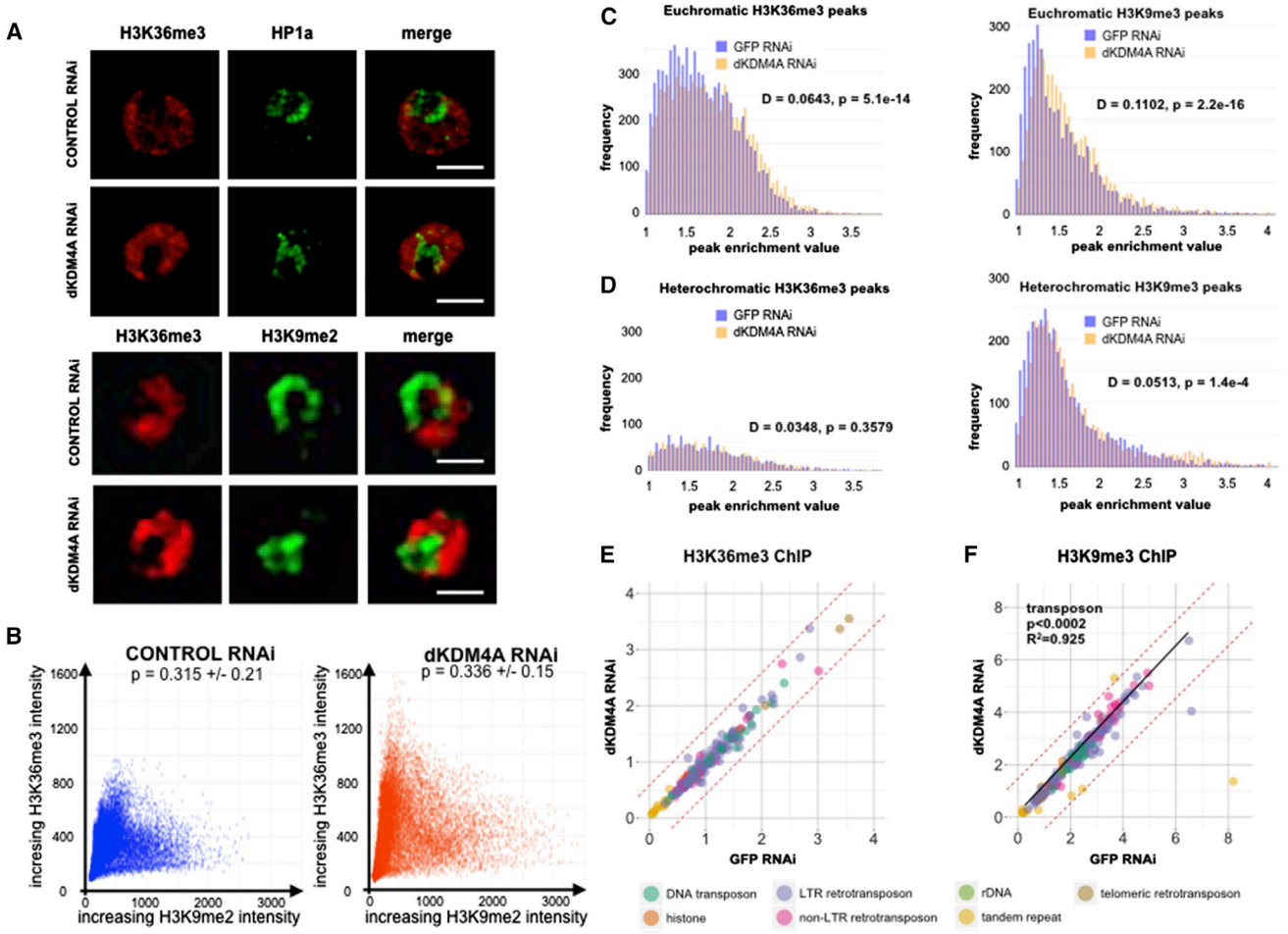

Figure 4. dKDM4A Demethylation of H3K36me3 Is Not a Significant Contributor to HP1a Domain Structure

(A) Representative IF images of Kc cells stained for H3K36me3 and HP1a (top) and H3K36me3 and H3K9me2 (bottom) after 5 days of y (control) or dKDM4A RNAi. Scale bars, 5 μm.

(B) Co-localization analysis of H3K36me3 and H3K9me2 signals after y or dKDM4A RNAi. Correlation coefficient, p, is shown, based on 23 cells.

(C and D) Histograms showing frequency distributions of H3K36me3 (left) and H3K9me3 (right) ChIP-seq peak enrichment values mapping to EC (C) and HC (D) after GFP control (blue) or dKDM4A (orange) RNAi. Data shown are cumulative peaks from two independent experiments, including p values and D-statistics from two-sample Kolmogorov-Smirnov test.

(E and F) Plots showing H3K36me3 (E) and H3K9me3 (F) enrichment values for repetitive elements between GFP and dKDM4A RNAi-treated cells (mean of two experiments). The SD of mean enrichment values (dotted lines) is used as a conservative measure of significantly increased or decreased association with H3K36me3 or H3K9me3 after dKDM4A depletion. In (F), a trendline drawn through the mean enrichment values of transposon sequences and a two-tailed t test highlight H3K9me3 enrichment after dKDM4A RNAi.

upon dKDM4A loss, rather than a direct defect in H3K9me3 demethylation.

dKDM4A Effects on PEV Do Not Require Its Catalytic Activity

Our results thus far suggest that dKDM4A effects on PEV are associated with a loss of repetitive DNA organization (Figures 2C–2E) and perturbations in H3K9me3 distributions in HC (Figures 4D and 4F). However, a key question that remains is whether dKDM4A catalytic activity is required for PEV. We tested flies containing either wild-type dKDM4A or a mutation previously shown to disable its catalytic activity (Lin et al., 2008; Crona et al., 2013) for their ability to complement the silencing defect exhibited by homozygous dKDM4A deletion mutants. Interestingly, both wild-type and catalytic mutant dKDM4A restored silencing of a y^+ reporter gene inserted in the fourth chromosome (Figure 5A). Thus, we conclude that dKDM4A demethylase activity is not required to maintain HC integrity, and propose that the observed changes in H3K9 methylation levels after dKDM4A RNAi are likely indirect and not due to loss of dKDM4A H3K9me3 demethylase activity. Based on the non-catalytic contribution to PEV and widespread localization of dKDM4A in HC, we propose that dKDM4A affects gene silencing primarily by regulating HC structure.

Overexpression of HP1a and some HC proteins can enhance PEV, resulting in additional silencing of transgene expression (Eissenberg et al., 1992; Tschiersch et al., 1994). We find that an extra copy of dKDM4A or of its catalytic mutant further

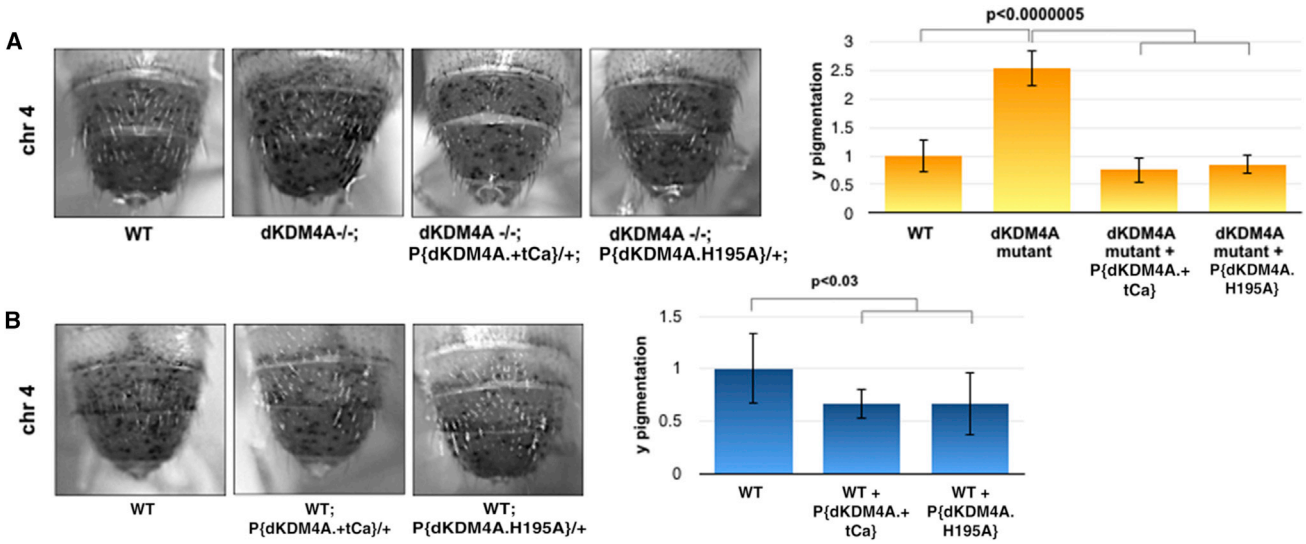

Figure 5. dKDM4A Enhances Variegation Independent of Its Catalytic Activity

(A) Representative images of y^+ PEV suppression between dKDM4A mutant flies expressing a single copy of wild-type (WT) or catalytically inactive dKDM4A transgene, and wild-type and dKDM4A mutant flies bearing no transgenes. Fiji-based quantitation of pigmentation levels of the two posterior segments is shown on the right, with Student's t test.

(B) Representative images of y^+ PEV suppression in wild-type flies with or without a single copy of wild-type or catalytically inactive dKDM4A transgene. Corresponding quantitation of pigmentation levels with Student's t test is shown.

Error bars represent SD. See also Figure S4.

silences y^+ inserted in HC of a wild-type background (Figure 5B), indicating that dKDM4A, like HP1a, is a triplo-enhancer of variegation. This result also further demonstrates that dKDM4A promotes HC silencing in a non-catalytic manner.

We also investigated a previous report showing that GAL-based overexpression of dKDM4A results in HP1a mislocalization from the chromocenter (Lin et al., 2008) by testing the variegation effects of GAL-overexpressed dKDM4A. Surprisingly, we observed that GAL-based overexpression of wild-type dKDM4A results in derepression of y^+ inserted in HC, but not overexpression of a dKDM4A PxVxL mutant incapable of binding HP1a (Figure S4). Thus, derepression of HC in response to high levels of dKDM4A is largely due to dKDM4A outcompeting other HC proteins that bind HP1a, which requires auxiliary factors to efficiently bind H3K9me3 (Eskeland et al., 2007). We conclude that an extra copy of dKDM4A enhances HC PEV, but extremely high levels of dKDM4A can interfere with proper HC structure, further indicating that dKDM4A dosage is critical for HC function.

dKDM4A Is Required for Normal Repair and Relocalization of Heterochromatic DSBs

Although the demethylase activity of dKDM4A is not required for PEV, it could be required for other HC functions. Su(var)3–9, which is critical for PEV and organization of repetitive DNA, is also required for normal repair of heterochromatic DSBs. We therefore tested dKDM4A for effects on the distinct spatiotemporal dynamics of heterochromatic DSBs induced after radiation treatment (IR). γH2Av foci that mark DSBs form rapidly within the DAPI-bright region of HC, then eventually relocalize to outside the HC domain (~30 min after IR). Loss of HC proteins (Su(var) 3–9, HP1a, and the SMC5/6 complex) blocks DSB relocalization, resulting in accumulation of γH2Av foci inside HC 60 min after IR (Chiolo et al., 2011).

Quantitation of γH2Av foci inside the DAPI-bright region at different time points after IR showed that cells depleted for dKDM4A accumulated higher levels of γH2Av foci than control cells 30–60 min after IR, similar to levels observed after HP1a depletion (Figure 6A). We conclude that dKDM4A is required for the normal DNA damage response in HC, specifically the relocalization of DSBs outside the HC domain. Although the frequency of γH2Av foci remaining in HC after dKDM4A depletion is still significantly higher than that in controls at 240 min after IR, they are significantly less than observed after HP1a RNAi (Figure 6A). This suggests that the requirement for dKDM4A in DSB relocalization is partially ameliorated at later time points after damage induction, which is not observed for HP1a, or that low levels of dKDM4A remaining after RNAi are sufficient to drive delayed DSB relocalization.

To identify a mechanism for dKDM4A-mediated repair of heterochromatic DSBs, we determined the role of dKDM4A enzymatic activity in DSB relocalization by measuring retention of γH2Av foci in HC in cells expressing only a catalytic mutant of dKDM4A. Kc cells stably expressing GFP-tagged wild-type or mutant dKDM4A constructs containing alternative codons were depleted for y (control) or endogenous dKDM4A (Figure 6B). As expected, we detected no retention of γH2Av foci in cells expressing the wild-type construct in the presence or absence of endogenous dKDM4A, compared with controls. However, cells expressing the dKDM4A catalytic mutant exhibited significantly higher levels of γH2Av foci retention in HC when endogenous dKDM4A was depleted (Figure 6C). These results show that dKDM4A-dependent demethylation is required for DSB relocalization in HC.

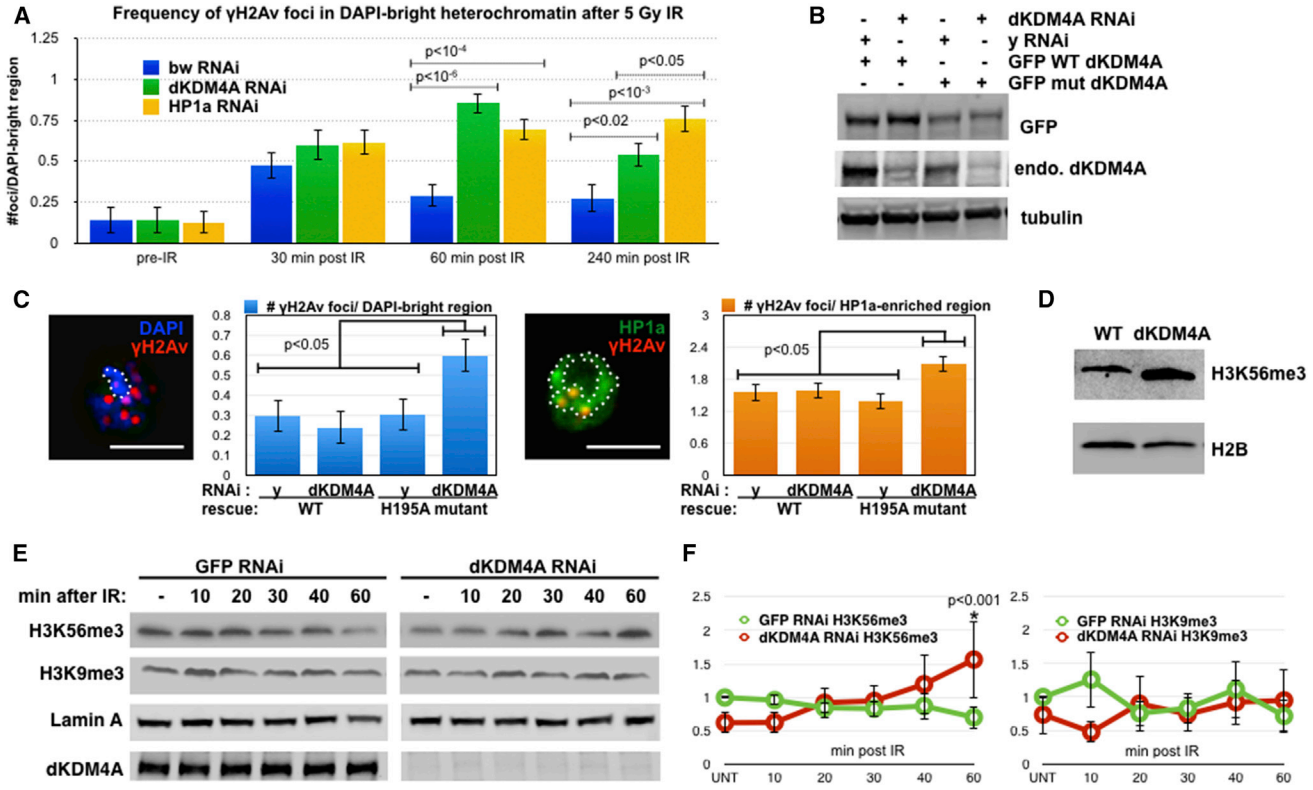

Figure 6. dKDM4A Is Required for Efficient Repair of Heterochromatic DNA Damage

(A) Graph comparing γH2Av foci frequency at DAPI-bright region between Kc cells after 5-day RNAi of bw (control), dKDM4A, or HP1a, and multiple time points after 5 Gy of IR. Error bars represent SE from two independent experiments.

(B) Western blot analysis of Kc cells stably expressing GFP-tagged wild-type or catalytically inactive dKDM4A transgenes with alternative codons after 5-day RNAi depletion of endogenous dKDM4A.

(C) Representative IF images of the same Kc cells showing retention of γH2Av foci in the heterochromatic DAPI-bright region (left, dotted line) and in HP1a-enriched HC (right, dotted line) 60 min after 5 Gy of IR. Scale bars, 5 μm. Quantitation of γH2Av foci frequency for each HC domain is shown to the right of each image, with Student's t test.

(D) Western blot showing H3K56me3 and H2B levels in larval extracts from dKDM4A mutant flies or wild-type (WT) flies.

(E) Representative western blots of Kc nuclear extracts after 5 days of GFP (control) or dKDM4A RNAi, and up to 60 min after 5 Gy of IR, showing H3K56me3, H3K9me3, dKDM4A, and Lamin levels.

(F) Quantitation of H3K56me3 and H3K9me3 levels in GFP or dKDM4A RNAi-treated cells post IR, after normalization to Lamin levels. Error bars indicate SE based on four independent experiments, and p value is based on Wilcoxon's rank test.

See also Figure S5.

We conclude that dKDM4A is required for relocalization of induced DSBs outside the HC domain, and consequently for the completion of repair when damage is induced by IR. Furthermore, the catalytic activity of dKDM4A is required for DSB mobilization, suggesting that lysine demethylation of one or more HC components is critical for proper DNA repair.

dKDM4A Is Required for Demethylation of H3K56me3 during DNA Damage

To identify a mechanism for dKDM4A enzymatic activity on heterochromatic DSB relocalization, we assayed several potential substrates for changes during DNA damage in HC. Based on recent results implicating H3K36me3 in DNA repair (Pai et al., 2014; Pfister et al., 2014), we first determined whether loss of dKDM4A results in increased H3K36me3 levels specifically at HC γH2Av foci after IR. Since loss of dKDM4A does not appreciably increase H3K36me3 levels in HC (Figure 4A), we performed co-IF staining of H3K36me3 at γH2Av foci within HP1a domains. Our results showed that γH2Av foci within HP1a domains are associated with low levels of H3K36me3 independently of the presence or absence of dKDM4A (Figure S5A). Therefore, the requirement for dKDM4A enzymatic activity during DSB relocalization in HC is not due to demethylation of H3K36me3, suggesting the presence of other substrates involved in DSB relocation.

We therefore tested whether DNA damage induced changes in overall levels of other potential dKDM4A substrates, such as H3K9me3 and H3K56me3, a recently discovered HC-enriched modification. Mammalian KDM4D and KDM4E were previously shown to demethylate H3K56me3 (Jack et al., 2013), but dKDM4A was not known to regulate this modification. Extracts of dKDM4A mutant flies showed accumulation of H3K56me3 compared with wild-type flies (Figure 6D), indicating that H3K56me3 is a potential substrate of dKDM4A during DNA

Table 1. dKDM4A Mutants Require Repair and Checkpoint Genes for Viability/Fertility

Protein	Mutant Genotype	Fertility	Viability* (%)	p Value <0.05*
	+; *dKDM4A*[*NP0618*]	fertile	100	NA
ATR	*mei41*[*29D*]; *dKDM4A*[*NP0618*]	sterile	17	+
	mei41[*D3*]; *dKDM4A*[*NP0618*]	sterile	16	+
MDC1	*mu2*[*1*]; *dKDM4A*[*NP0618*]	sterile	57	+
TOPBP1	*mus101*[*D1*]; *dKDM4A*[*NP0618*]	fertile	80	+
NBS1	*nbs1*[*1*]/+; *dKDM4A*[*NP0618*]	ND	82	+
ATM	*tefu*[*8*]/+; *dKDM4A*[*NP0618*]	fertile	97	–
SMC1	*SMC1*[*exc46*]/+; *dKDM4A*[*NP0618*]	ND	82	–
Rod	*rod*[*EY04576*]; *dKDM4A*[*NP0618*]	ND	84	–
Zw10	*zw10*[*5*]/+; *dKDM4A*[*NP0618*]	ND	98	–

Viability and fertility of mutant dKDM4A flies is compared with double mutants for dKDM4A and genes involved in DNA repair/DNA damage checkpoint: *mei-41* (ATR), *mu2* (MDC1), *mus101* (TOPBP1), *nbs1*, *tefu* (ATM); cohesion: *SMC1*; and mitotic checkpoint: *rod* and *zw10*. *An adjusted percent viability (see STAR Methods) is shown due to the partial lethality of homozygous dKDM4A mutants and is used to calculate Student's t test. ND, not determined. See also Table S3.

repair. Interestingly, analysis of Kc cell extracts after IR showed that global H3K56me3 levels decreased after DNA damage in control cells, but increased in cells depleted for dKDM4A 30 min after IR treatment (Figures 6E and 6F). Thus, H3K56me3 levels normally increase after DNA damage, but are quickly reduced by KDM4A-mediated demethylation. In contrast, H3K9me3 levels are not altered by the presence or absence of dKDM4A (Figures 6D and 6E), indicating that H3K56me3 levels are specifically modulated by dKDM4A during DNA repair. Moreover, H3K56me3 levels in the absence of dKDM4A start increasing at 30 min after IR, coinciding with the timing of normal DSB relocalization and aberrant γH2Av foci retention in HC in mutants (Figure 6A). Finally, IF staining showed that H3K56me3 remained heavily enriched in HP1a-bound HC in the presence or absence of dKDM4A, with and without DNA damage (Figure S5B), and did not specifically overlap with or change at γH2Av foci (Figure S5C). Thus IR-induced changes in H3K56me3 levels may occur throughout HC, and not specifically at sites of DSBs. Alternatively, local changes in H3K56me3 levels are not readily detectable in HC by IF staining or may occur only upon exit of DSBs from HC.

Further analysis revealed that Su(var)3–9 RNAi nearly abrogates H3K56me3 levels in *Drosophila*, as previously shown in mammals and worms (Jack et al., 2013), and prevented the accumulation of H3K56me3 after IR (Figure S5D). This suggests that Su(var)3–9 is the HMTase responsible for the increased levels of H3K56me3 observed after IR, in the absence of dKDM4A (Figures 6D and 6E). We therefore propose that H3K56me3 is a new substrate involved in HC DSB repair, which is catalyzed by Su(var)3–9 and demethylated by dKDM4A after DNA damage.

dKDM4A Mutants Are Synthetically Lethal when Combined with Mutations in Checkpoint or Repair Genes

The involvement of dKDM4A in DNA repair and genome stability was further evaluated by determining whether synthetic lethality or sterility occurs when dKDM4A mutations are combined with cell-cycle checkpoint or repair mutations, as observed previously for *Su(var)3–9* null mutations (Peng and Karpen, 2009). Ratios were normalized to account for the slight subviability of homozygous dKDM4A null mutant adults (see STAR Methods) (Table S3A). Homozygous dKDM4A mutants showed statistically significant synthetic lethality and/or sterility when combined with mutations in ATR (checkpoint), Mdc1/mu2, TOPBP1, and NBS1 (repair), but not ATM (Table 1). A second dKDM4A mutant displayed similar subviability among homozygotes (Table S3A) and synthetic lethality with ATR (Table S3B). We further compared the viability of a dKDM4A, ATR double mutant with siblings that express either wild-type or catalytically inactive dKDM4A transgenes. The wild-type dKDM4A transgene rescued the lethality of the dKDM4A, ATR double mutant, whereas the catalytically inactive dKDM4A transgene increased lethality (Table 2), suggesting that expression of the mutated dKDM4A transgene induces dominant-negative effects. These findings demonstrate that dKDM4A plays an important role in the repair of heterochromatic DSBs, consistent with our results showing that dKDM4A enzymatic activity is required for DSB relocalization from HC.

We conclude that complete loss of dKDM4A generates high enough levels of spontaneous DNA damage or defective repair to require ATR, Mdc1, TOPBP1, and NBS1 for organismal survival or fertility. However, unlike Su(var)3–9, dKDM4A mutants did not display synthetic lethality with mutants for the mitotic checkpoint (*rod* or *zw10*) or the cohesin SMC1 (Peng and Karpen, 2009). In fact, dKDM4A, Su(var)3–9 double mutants display similar viability as Su(var)3–9 null mutants, but have lower viability than dKDM4A mutants (Table S3C, D). This suggests that (1) dKDM4A and Su(var)3–9 act in the same pathway governing genome stability, and (2) the additional requirement of Su(var)3–9 for normal chromosome segregation (Peng and Karpen, 2009) is responsible for the lower viability of Su(var)3–9 mutants compared with dKDM4A mutants. We conclude that dKDM4A ensures genome stability by promoting normal HC DNA repair and not chromosome segregation.

DISCUSSION

Our investigations show that *Drosophila* KDM4A is a structural component of HC, and regulates HC organization, PEV, and DNA repair (Figures S6A–S6C). This study also identifies distinct

Table 2. dKDM4A Catalytic Site Is Required for Viability of ATR Mutant

Genotype	Viability* (%)	p Value <0.05*
mei41[29D]/+; Δ*dKDM4A*/+	100	NA
mei41[29D]/+; Δ*dKDM4A*/+; *P{dKDM4A.+tCa}*/+	235	+
mei41[29D]/+; Δ*dKDM4A*/+; *P{dKDM4A.H195A}*/+	67	+

Viability of double heterozygotes for ATR and dKDM4A mutations is compared with siblings containing either a wild-type or catalytic mutant dKDM4A transgene. *An adjusted percent viability (see STAR Methods) is shown due to the partial lethality of homozygous dKDM4A mutants and is used to calculate Student's t test. See also Table S3.

dKDM4A functions in different nuclear domains (HC versus EC) and both structural and catalytic dKDM4A roles in HC, highlighting the significance of determining the enzymatic and non-enzymatic roles of dKDM4A homologs and their diversity in function and localization. dKDM4A is recruited to HC downstream of HP1a and Su(var)3–9, and is required for PEV in a non-catalytic manner. This suggests that dKDM4A contributes structurally to gene silencing and regulates the proper organization of HC complexes and sequences (Figure S6B). dKDM4A is also required for relocalization and proper repair of heterochromatic DSBs (Figure S6C). Intriguingly, normal HC DSB dynamics depend on dKDM4A catalytic activity and are associated with dKDM4A-dependent H3K56me3 demethylation, suggesting that this HC mark and its demethylated state(s) are important for DNA repair. Moreover, dKDM4A is required for organismal survival in the presence of mutations disrupting DNA repair and checkpoint pathways, further supporting a key role for this protein in maintaining genome stability.

The observation that dKDM4A is required for higher-order HC structure, specifically the organization of satellite DNAs, suggests that dKDM4A functions to maintain HC architecture. However, such defects in HC structure caused by loss of dKDM4A do not result from visible disruption of HP1a localization or dynamics, or from altered H3K36me3 levels in HC. Although we detected changes in H3K9me3 levels after loss of dKDM4A, these were not sufficient to alter transcription of the majority of HC elements. Whether dKDM4A directly or indirectly affects H3K9me3 levels *in vivo* is unclear. Regardless, we show that PEV does not require dKDM4A enzymatic activity, indicating that HC-mediated gene silencing is not directly regulated by dKDM4A demethylation of H3K9me3, or any other substrate. Although it is possible that the minor H3K9me3 perturbations are sufficient to disrupt HC, these results are more consistent with a direct structural role for dKDM4A in HC organization and gene silencing.

dKDM4A is directly recruited to HC by HP1a, suggesting that dKDM4A closely participates in HP1a-mediated HC functions. dKDM4A effects on variegation indicate that recruitment of factors downstream of HP1a assembly are required for full HC integrity and function. Although dKDM4A is not required for HP1a-mediated suppression of transposable element transcription, we detect dKDM4A-dependent effects on satellite repeat organization. This could suggest that suppression of PEV by dKDM4A mutants results from disruption of higher-order HC structure that increases accessibility of transcriptional machinery to HC domains. FISH studies have identified a host of regulatory proteins, including cohesins and condensins, that promote or antagonize pairing between HC domains (Joyce et al., 2012). Whether dKDM4A participates in chromosome pairing, or influences cohesion or condensation in HC, remains to be determined. Alternatively, dKDM4A may assemble or link repetitive sequences into discrete domains within HC, which become unraveled and dispersed in the absence of dKDM4A, or dKDM4A may protect repetitive regions from being excised as extrachromosomal circles (Peng and Karpen, 2007).

A role in genome organization could also account for the impact of dKDM4A on HC DNA repair. Impaired repair of IR-induced DSBs in the absence of dKDM4A could result from defects in pairing of homologous chromosomes or sister chromatids, which would normally facilitate "safe" HR among repeats, or from problems in folding or concatenation of HC domains that inhibit efficient exit of repair foci from HC. In fact, homozygous dKDM4A mutant adult flies are underrepresented compared with their heterozygote siblings; improper repair of spontaneous DNA breaks in HC could account for this subviability. This is consistent with observations in *Caenorhabditis elegans*, where loss of the dKDM4A homolog results in impaired DNA replication, accumulation of DNA damage, and increased apoptosis (Black et al., 2010).

Support for this hypothesis comes from the synthetic lethality and infertility observed when a dKDM4A mutation is combined with mutations in the DNA damage checkpoint/DNA repair pathways, but not components of the mitotic checkpoint. Thus, spontaneous DNA damage requires dKDM4A to regulate HC structure for efficient repair. Su(var)3–9, but not dKDM4A, is also synthetically lethal with mitotic checkpoint mutants (Peng and Karpen, 2009), which may reflect a higher level of spontaneous breaks that occur in the absence of Su(var)3–9, or defects in cohesin recruitment (Peng and Karpen, 2009). This suggests that HC affects multiple pathways controlling genome stability, of which a subset is regulated by dKDM4A.

Our experiments also identify a close relationship between dKDM4A and HP1a. HP1a directly recruits dKDM4A to HC, and dKDM4A overexpression can effectively sequester HP1a away from HC (Lin et al., 2008), which we show results in suppression of PEV. dKDM4A overexpression also potentially excludes other HP1a CSD-binding partners from HC, which could further exacerbate effects on HC functions. We also identified EC genes that are co-regulated by dKDM4A and HP1a (Figure S6A), indicating that even outside the HC domain these two proteins function together. This result contrasts with previously published data showing antagonistic effects of dKDM4A and HP1a on transcription (Crona et al., 2013), and may reflect the differences between immediate RNAi effects on tissue culture cells and steady-state effects that develop in mutant fly tissues.

Previously, HP1a binding was shown to enhance the H3K36me3 demethylase activity of dKDM4A (Lin et al., 2008). However, our results suggest that dKDM4A does not exert PEV regulatory effects through demethylase activity and is not responsible for the low H3K36me3 levels in HC. Therefore, HP1a stimulation of dKDM4A H3K36me3 likely occurs in EC genes, although we cannot exclude the possibility that local

H3K36me3 levels increase at a few HC genes (Lin et al., 2012). Instead we propose that the primary role of dKDM4A in HC is to ensure normal assembly of HP1a complexes that drives HC organization/structure and PEV.

A primarily structural role for dKDM4A in HC does not preclude the possibility that its catalytic activity regulates other HC functions. In fact, we show that dKDM4A enzymatic activity is required for DSBs to relocalize from HC, suggesting that a demethylated substrate facilitates HC repair dynamics and completion of DNA repair. Of three potential histone substrates tested, we identified H3K56me3, which is enriched in HC and is demethylated by a dKDM4A homolog (KDM4D) in mammals (Jack et al., 2013), as accumulating in the absence of dKDM4A, specifically after DNA damage induction by IR and in a Su(var)3–9-dependent manner. In mammals, KDM4D transiently localizes to DNA damage sites (Khoury-Haddad et al., 2014), but whether KDM4D demethylates H3K56me3 during DNA damage remains to be determined. Little is known about H3K56me3 function, but this residue resides at the junction between histone H3 and nucleosomal DNA and could regulate unfolding of DNA from the nucleosome (Luger et al., 1997). H3K56me3 demethylation also occurs during replication in mammalian cells (Jack et al., 2013), suggesting that the replication machinery requires removal of this mark for access to HC. Similarly, H3K56me3 demethylation by dKDM4A could also facilitate chromatin changes required for DSB relocalization and successful DNA repair.

Alternatively, the requirement for dKDM4A enzymatic activity in DSB relocalization may involve demethylation of other histone and non-histone proteins. Methylated peptides found in various non-histone chromatin proteins have been shown to be demethylated by a mammalian KDM4A homolog (Ponnaluri et al., 2009). Moreover, a fission yeast homolog lacking demethylase activity functions as an anti-silencing factor in HC, and has been proposed to act as a protein hydroxylase (Trewick et al., 2007). Therefore, we propose that dKDM4A recruitment to HC by HP1a regulates heterochromatic DSB repair and genome stability through demethylation of HC-specific mark(s), such as H3K56me3, but could also involve demethylation or hydroxylation of other HC components.

Many cancers acquire abnormal levels of HC components, which may increase genome instability and promote misregulation of oncogenes and tumor suppressors (Carone and Lawrence, 2013; Choi and Lee, 2013). Overexpression of several KDM4A family members has been shown to correlate with and drive tumor progression (Berry and Janknecht, 2013). Although it remains to be determined if human KDM4A family members regulate HC structure and promote HC DNA repair, disruption of such functions potentially contributes to tumorigenesis. Our findings therefore expand our understanding of how this demethylase family exerts a myriad of effects in cancer tissue. Overexpression/ectopic expression of human KDM4A homologs have been shown to induce transient site-specific amplification of a cytogenetic region containing satellite DNA in tumors and cell lines (Black et al., 2013), antagonize 53BP1 binding to DSBs (Mallette et al., 2012), disrupt mismatch repair (Awwad and Ayoub, 2015), and produce chromosomal instability (Slee et al., 2012) and chromosome missegregation (Kupershmit et al., 2014). Further studies are required to determine whether high levels of KDM4A homologs promote tumor progression solely through altered transcriptional regulation of EC cancer-linked genes, or whether defects in HC structure and function also advance genomic evolution of cancers.

STAR★METHODS

Detailed methods are provided in the online version of this paper and include the following:

- KEY RESOURCES TABLE
- CONTACT FOR REAGENT AND RESOURCE SHARING
- EXPERIMENTAL MODEL AND SUBJECT DETAILS
- METHOD DETAILS
  - Plasmid Construction
  - Fly Lines
  - Tissue Culture Manipulation
  - FISH and Immunofluorescence
  - RNA-Seq and ChIP-Seq
  - Sequencing Analysis
  - Western Blotting
- QUANTIFICATION AND STATISTICAL ANALYSIS
  - Fly Viability
  - ChIP-Seq and RNA-Seq
  - Western Blotting
  - Image Analysis
- DATA AND SOFTWARE AVAILABILITY

SUPPLEMENTAL INFORMATION

Supplemental Information includes six figures and four tables and can be found with this article online at http://dx.doi.org/10.1016/j.devcel.2017.06.014.

AUTHOR CONTRIBUTIONS

Conceptualization, S.U.C. and G.H.K.; Methodology, S.U.C., J.M.S., S.A.L., and G.H.K.; Software, S.A.L., C.K., and S.V.C.; Validation, S.U.C., J.M.S., and S.A.L.; Formal Analysis, S.U.C., J.M.S., and S.A.L.; Investigation, S.U.C.; Resources, S.A.L., S.V.C., and G.H.K.; Writing – Original Draft, S.U.C. and G.H.K.; Writing – Review & Editing, S.U.C., J.M.S., and G.H.K.; Visualization, S.U.C.; Supervision, S.U.C. and G.H.K.; Project Administration, S.U.C. and G.H.K.; Funding Acquisition, S.U.C. and G.H.K.

ACKNOWLEDGMENTS

The authors thank: R. Scott Hawley, Mattias Mannervik, Gunter Reuter, Tin Tin Su, and Jerry L. Workman for fly stocks; Sandra B. Hake for the H3K56me3 antibody; Barbara G. Mellone, Ann Kim, and W. Kyle Mills for plasmids; Irene Chiolo, Aki Minoda, Aniek Janssen, and Nicole L. Beier for experimental guidance; and Aniek Janssen, Grace Y.C. Lee, and Weiguo Zhang for critical comments on the manuscript. This work was supported by the Ruth Kirchstein NIH Postdoctoral Fellowship (1F32GM086111) and Laboratory Directed Research and Development Program (LB13037) to S.U.C. and NIH R01 grants R01 GM086613 and GM117420 to G.H.K.

Received: April 27, 2016
Revised: March 21, 2017
Accepted: June 16, 2017
Published: July 24, 2017

REFERENCES

Alekseyenko, A.A., Gorchakov, A.A., Zee, B.M., Fuchs, S.M., Kharchenko, P.V., and Kuroda, M.I. (2014). Heterochromatin-associated interactions of

Drosophila HP1a with dADD1, HIPP1, and repetitive RNAs. Genes Dev. *28*, 1445–1460.

Awwad, S.W., and Ayoub, N. (2015). Overexpression of KDM4 lysine demethylases disrupts the integrity of the DNA mismatch repair pathway. Biol. Open *4*, 498–504.

Bannister, A.J., Zegerman, P., Partridge, J.F., Miska, E.A., Thomas, J.O., Allshire, R.C., and Kouzarides, T. (2001). Selective recognition of methylated lysine 9 on histone H3 by the HP1 chromo domain. Nature *410*, 120–124.

Barigozzi, C., Dolfini, S., Fraccaro, M., Raimondi, G.R., and Tiepolo, L. (1966). In vitro study of the DNA replication patterns of somatic chromosomes of *Drosophila melanogaster*. Exp. Cell Res. *43*, 231–234.

Berry, W.L., and Janknecht, R. (2013). KDM4/JMJD2 histone demethylases: epigenetic regulators in cancer cells. Cancer Res. *73*, 2936–2942.

Black, J.C., Allen, A., Van Rechem, C., Forbes, E., Longworth, M., Tschop, K., Rinehart, C., Quiton, J., Walsh, R., Smallwood, A., et al. (2010). Conserved antagonism between JMJD2A/KDM4A and HP1gamma during cell cycle progression. Mol. Cell *40*, 736–748.

Black, J.C., Manning, A.L., Van Rechem, C., Kim, J., Ladd, B., Cho, J., Pineda, C.M., Murphy, N., Daniels, D.L., Montagna, C., et al. (2013). KDM4A lysine demethylase induces site-specific copy gain and rereplication of regions amplified in tumors. Cell *154*, 541–555.

Cann, K.L., and Dellaire, G. (2011). Heterochromatin and the DNA damage response: the need to relax. Biochem. Cell Biol. *89*, 45–60.

Carone, D.M., and Lawrence, J.B. (2013). Heterochromatin instability in cancer: from the Barr body to satellites and the nuclear periphery. Semin. Cancer Biol. *23*, 99–108.

Cheutin, T., McNairn, A.J., Jenuwein, T., Gilbert, D.M., Singh, P.B., and Misteli, T. (2003). Maintenance of stable heterochromatin domains by dynamic HP1 binding. Science *299*, 721–725.

Chiolo, I., Minoda, A., Colmenares, S.U., Polyzos, A., Costes, S.V., and Karpen, G.H. (2011). Double-strand breaks in heterochromatin move outside of a dynamic HP1a domain to complete recombinational repair. Cell *144*, 732–744.

Choi, J.D., and Lee, J.S. (2013). Interplay between epigenetics and genetics in cancer. Genomics Inform. *11*, 164–173.

Crona, F., Dahlberg, O., Lundberg, L.E., Larsson, J., and Mannervik, M. (2013). Gene regulation by the lysine demethylase KDM4A in *Drosophila*. Dev. Biol. *373*, 453–463.

Dinant, C., and Luijsterburg, M.S. (2009). The emerging role of HP1 in the DNA damage response. Mol. Cell. Biol. *29*, 6335–6340.

Egelhofer, T.A., Minoda, A., Klugman, S., Lee, K., Kolasinska-Zwierz, P., Alekseyenko, A.A., Cheung, M.S., Day, D.S., Gadel, S., Gorchakov, A.A., et al. (2011). An assessment of histone-modification antibody quality. Nat. Struct. Mol. Biol. *18*, 91–93.

Eissenberg, J.C., and Elgin, S.C. (2000). The HP1 protein family: getting a grip on chromatin. Curr. Opin. Genet. Dev. *10*, 204–210.

Eissenberg, J.C., James, T.C., Foster-Hartnett, D.M., Hartnett, T., Ngan, V., and Elgin, S.C. (1990). Mutation in a heterochromatin-specific chromosomal protein is associated with suppression of position-effect variegation in *Drosophila melanogaster*. Proc. Natl. Acad. Sci. USA *87*, 9923–9927.

Eissenberg, J.C., Morris, G.D., Reuter, G., and Hartnett, T. (1992). The heterochromatin-associated protein HP-1 is an essential protein in *Drosophila* with dosage-dependent effects on position-effect variegation. Genetics *131*, 345–352.

Elgin, S.C.R., and Reuter, G. (2013). Position-effect variegation, heterochromatin formation, and gene silencing in *Drosophila*. Cold Spring Harb. Perspect. Biol. *5*, a017780.

Eskeland, R., Eberharter, A., and Imhof, A. (2007). HP1 binding to chromatin methylated at H3K9 is enhanced by auxiliary factors. Mol. Cell. Biol. *27*, 453–465.

Fanti, L., Giovinazzo, G., Berloco, M., and Pimpinelli, S. (1998). The heterochromatin protein 1 prevents telomere fusions in *Drosophila*. Mol. Cell *2*, 527–538.

Grigliatti, T. (1991). Position-effect variegation—an assay for nonhistone chromosomal proteins and chromatin assembly and modifying factors. Methods Cell Biol. *35*, 587–627.

Guerra-Calderas, L., Gonzalez-Barrios, R., Herrera, L.A., Cantu de Leon, D., and Soto-Reyes, E. (2015). The role of the histone demethylase KDM4A in cancer. Cancer Genet. *208*, 215–224.

Heitz, E. (1928). Das Heterochromatin der Moose. Jahrb. Wiss. Bot. *69*, 762–818.

Hoskins, R.A., Carlson, J.W., Kennedy, C., Acevedo, D., Evans-Holm, M., Frise, E., Wan, K.H., Park, S., Mendez-Lago, M., Rossi, F., et al. (2007). Sequence finishing and mapping of *Drosophila melanogaster* heterochromatin. Science *316*, 1625–1628.

Jack, A.P.M., Bussemer, S., Hahn, M., Pünzeler, S., Snyder, M., Wells, M., Csankovszki, G., Solovei, I., Schotta, G., and Hake, S.B. (2013). H3K56me3 is a novel, conserved heterochromatic mark that largely but not completely overlaps with H3K9me3 in both regulation and localization. PLoS One *8*, e51765.

Joyce, E.F., Williams, B.R., Xie, T., and Wu, C.T. (2012). Identification of genes that promote or antagonize somatic homolog pairing using a high-throughput FISH-based screen. PLoS Genet. *8*, e1002667.

Karpen, G.H., and Allshire, R.C. (1997). The case for epigenetic effects on centromere identity and function. Trends Genetics *13*, 489–496.

Kellum, R., and Alberts, B.M. (1995). Heterochromatin protein 1 is required for correct chromosome segregation in *Drosophila* embryos. J. Cell Sci. *108*, 1419–1431.

Khoury-Haddad, H., Guttmann-Raviv, N., Ipenberg, I., Huggins, D., Jeyasekharan, A.D., and Ayoub, N. (2014). PARP1-dependent recruitment of KDM4D histone demethylase to DNA damage sites promotes double-strand break repair. Proc. Natl. Acad. Sci. USA *111*, E728–E737.

Klose, R.J., Yamane, K., Bae, Y., Zhang, D., Erdjument-Bromage, H., Tempst, P., Wong, J., and Zhang, Y. (2006). The transcriptional repressor JHDM3A demethylates trimethyl histone H3 lysine 9 and lysine 36. Nature *442*, 312–316.

Konev, A.Y., Yan, C.M., Acevedo, D., Kennedy, C., Ward, E., Lim, A., Tickoo, S., and Karpen, G.H. (2003). Genetics of P-element transposition into *Drosophila melanogaster* centric heterochromatin. Genetics *165*, 2039–2053.

Kupershmit, I., Khoury-Haddad, H., Awwad, S.W., Guttmann-Raviv, N., and Ayoub, N. (2014). KDM4C (GASC1) lysine demethylase is associated with mitotic chromatin and regulates chromosome segregation during mitosis. Nucleic Acids Res. *42*, 6168–6182.

Lander, E.S., Linton, L.M., Birren, B., Nusbaum, C., Zody, M.C., Baldwin, J., Devon, K., Dewar, K., Doyle, M., FitzHugh, W., et al. (2001). Initial sequencing and analysis of the human genome. Nature *409*, 860–921.

Langmead, B., Trapnell, C., Pop, M., and Salzberg, S.L. (2009). Ultrafast and memory-efficient alignment of short DNA sequences to the human genome. Genome Biol. *10*, R25.

Laurencon, A., Purdy, A., Sekelsky, J., Hawley, R.S., and Su, T.T. (2003). Phenotypic analysis of separation-of-function alleles of MEI-41, *Drosophila* ATM/ATR. Genetics *164*, 589–601.

Li, H., Handsaker, B., Wysoker, A., Fennell, T., Ruan, J., Homer, N., Marth, G., Abecasis, G., and Durbin, R.; Genome Project Data Processing Subgroup (2009). The Sequence Alignment/Map format and SAMtools. Bioinformatics *25*, 2078–2079.

Lin, C.-H., Li, B., Swanson, S., Zhang, Y., Florens, L., Washburn, M.P., Abmayr, S.M., and Workman, J.L. (2008). Heterochromatin protein 1a stimulates histone H3 lysine 36 demethylation by the *Drosophila* KDM4A demethylase. Mol. Cell *32*, 696–706.

Lin, C.H., Paulson, A., Abmayr, S.M., and Workman, J.L. (2012). HP1a targets the *Drosophila* KDM4A demethylase to a subset of heterochromatic genes to regulate H3K36me3 levels. PLoS One *7*, e39758.

Lloret-Llinares, M., Carré, C., Vaquero, A., de Olano, N., and Azorín, F. (2008). Characterization of *Drosophila melanogaster* JmjC+N histone demethylases. Nucleic Acids Res. *36*, 2852–2863.

Lorbeck, M.T., Singh, N., Zervos, A., Dhatta, M., Lapchenko, M., Yang, C., and Elefant, F. (2010). The histone demethylase Dmel\Kdm4A controls genes

required for life span and male-specific sex determination in *Drosophila*. Gene *450*, 8–17.

Love, M.I., Huber, W., and Anders, S. (2014). Moderated estimation of fold change and dispersion for RNA-seq data with DESeq2. Genome Biol. *15*, 550.

Luger, K., Mader, A.W., Richmond, R.K., Sargent, D.F., and Richmond, T.J. (1997). Crystal structure of the nucleosome core particle at 28 A resolution. Nature *389*, 251–260.

Mallette, F.A., Mattiroli, F., Cui, G., Young, L.C., Hendzel, M.J., Mer, G., Sixma, T.K., and Richard, S. (2012). RNF8- and RNF168-dependent degradation of KDM4A/JMJD2A triggers 53BP1 recruitment to DNA damage sites. EMBO J. *31*, 1865–1878.

Nottke, A., Colaiacovo, M.P., and Shi, Y. (2009). Developmental roles of the histone lysine demethylases. Development *136*, 879–889.

Pai, C.C., Deegan, R.S., Subramanian, L., Gal, C., Sarkar, S., Blaikley, E.J., Walker, C., Hulme, L., Bernhard, E., Codlin, S., et al. (2014). A histone H3K36 chromatin switch coordinates DNA double-strand break repair pathway choice. Nat. Commun. *5*, 4091.

Peng, J.C., and Karpen, G.H. (2007). H3K9 methylation and RNA interference regulate nucleolar organization and repeated DNA stability. Nat. Cell Biol. *9*, 25–35.

Peng, J.C., and Karpen, G.H. (2009). Heterochromatic genome stability requires regulators of histone H3 K9 methylation. PLoS Genet. *5*, e1000435.

Pfister, S.X., Ahrabi, S., Zalmas, L.P., Sarkar, S., Aymard, F., Bachrati, C.Z., Helleday, T., Legube, G., La Thangue, N.B., Porter, A.C., et al. (2014). SETD2-dependent histone H3K36 trimethylation is required for homologous recombination repair and genome stability. Cell Rep. *7*, 2006–2018.

Piacentini, L., and Pimpinelli, S. (2010). Positive regulation of euchromatic gene expression by HP1. Fly *4*, 1–3.

Ponnaluri, V.K., Vavilala, D.T., Putty, S., Gutheil, W.G., and Mukherji, M. (2009). Identification of non-histone substrates for JMJD2A-C histone demethylases. Biochem. Biophys. Res. Commun. *390*, 280–284.

Rangan, P., Malone, C.D., Navarro, C., Newbold, S.P., Hayes, P.S., Sachidanandam, R., Hannon, G.J., and Lehmann, R. (2011). piRNA production requires heterochromatin formation in *Drosophila*. Curr. Biol. *21*, 1373–1379.

Riddle, N.C., Minoda, A., Kharchenko, P.V., Alekseyenko, A.A., Schwartz, Y.B., Tolstorukov, M.Y., Gorchakov, A.A., Jaffe, J.D., Kennedy, C., Linder-Basso, D., et al. (2011). Plasticity in patterns of histone modifications and chromosomal proteins in *Drosophila* heterochromatin. Genome Res. *21*, 147–163.

Ryu, H.-W., Lee, D.H., Florens, L., Swanson, S.K., Washburn, M.P., and Kwon, S.H. (2014). Analysis of the heterochromatin protein 1 (HP1) interactome in *Drosophila*. J. Proteomics *102*, 137–147.

Ryu, T., Spatola, B., Delabaere, L., Bowlin, K., Hopp, H., Kunitake, R., Karpen, G.H., and Chiolo, I. (2015). Heterochromatic breaks move to the nuclear periphery to continue recombinational repair. Nat. Cell Biol. *17*, 1401–1411.

Savitsky, M., Kravchuk, O., Melnikova, L., and Georgiev, P. (2002). Heterochromatin protein 1 is involved in control of telomere elongation in *Drosophila melanogaster*. Mol. Cell. Biol. *22*, 3204–3218.

Schindelin, J., Arganda-Carreras, I., Frise, E., Kaynig, V., Longair, M., Pietzsch, T., Preibisch, S., Rueden, C., Saalfeld, S., Schmid, B., et al. (2012). Fiji: an open-source platform for biological-image analysis. Nat. Methods *9*, 676–682.

Schotta, G., Ebert, A., Krauss, V., Fischer, A., Hoffmann, J., Rea, S., Jenuwein, T., Dorn, R., and Reuter, G. (2002). Central role of *Drosophila* SU(VAR)3-9 in histone H3-K9 methylation and heterochromatic gene silencing. EMBO J. *21*, 1121–1131.

Schotta, G., Ebert, A., Dorn, R., and Reuter, G. (2003). Position-effect variegation and the genetic dissection of chromatin regulation in *Drosophila*. Semin. Cell Dev. Biol. *14*, 67–75.

Schuldiner, O., Berdnik, D., Levy, J.M., Wu, J.S., Luginbuhl, D., Gontang, A.C., and Luo, L. (2008). piggyBac-based mosaic screen identifies a postmitotic function for cohesin in regulating developmental axon pruning. Dev. Cell *14*, 227–238.

Seum, C., Reo, E., Peng, H., Rauscher, F.J., 3rd, Spierer, P., and Bontron, S. (2007). *Drosophila* SETDB1 is required for chromosome 4 silencing. PLoS Genet. *3*, e76.

Sibon, O.C., Laurencon, A., Hawley, R., and Theurkauf, W.E. (1999). The *Drosophila* ATM homologue Mei-41 has an essential checkpoint function at the midblastula transition. Curr. Biol. *9*, 302–312.

Slee, R.B., Steiner, C.M., Herbert, B.-S., Vance, G.H., Hickey, R.J., Schwarz, T., Christan, S., Radovich, M., Schneider, B.P., Schindelhauer, D., et al. (2012). Cancer-associated alteration of pericentromeric heterochromatin may contribute to chromosome instability. Oncogene *31*, 3244–3253.

Swenson, J.M., Colmenares, S.U., Strom, A.R., Costes, S.V., and Karpen, G.H. (2016). The composition and organization of *Drosophila* heterochromatin are heterogeneous and dynamic. Elife *5*, e16096, http://dx.doi.org/10.7554/eLife.16096.

Trapnell, C., Roberts, A., Goff, L., Pertea, G., Kim, D., Kelley, D.R., Pimentel, H., Salzberg, S.L., Rinn, J.L., and Pachter, L. (2012). Differential gene and transcript expression analysis of RNA-seq experiments with TopHat and Cufflinks. Nat. Protoc. *7*, 562–578.

Trewick, S.C., Minc, E., Antonelli, R., Urano, T., and Allshire, R.C. (2007). The JmjC domain protein Epe1 prevents unregulated assembly and disassembly of heterochromatin. EMBO J. *26*, 4670–4682.

Trojer, P., Zhang, J., Yonezawa, M., Schmidt, A., Zheng, H., Jenuwein, T., and Reinberg, D. (2009). Dynamic histone H1 Isotype 4 methylation and demethylation by histone lysine methyltransferase G9a/KMT1C and the Jumonji domain-containing JMJD2/KDM4 Proteins. J. Biol. Chem. *284*, 8395–8405.

Tschiersch, B., Hofmann, A., Krauss, V., Dorn, R., Korge, G., and Reuter, G. (1994). The protein encoded by the *Drosophila* position-effect variegation suppressor gene Su(var)3-9 combines domains of antagonistic regulators of homeotic gene complexes. EMBO J. *13*, 3822–3831.

Tsurumi, A., Dutta, P., Shang, R., Yan, S.J., and Li, W.X. (2013). *Drosophila* Kdm4 demethylases in histone H3 lysine 9 demethylation and ecdysteroid signaling. Sci. Rep. *3*, 2894.

Weiler, K.S., and Wakimoto, B.T. (1995). Heterochromatin and gene expression in *Drosophila*. Annu. Rev. Genet. *29*, 577–605.

Whetstine, J.R., Nottke, A., Lan, F., Huarte, M., Smolikov, S., Chen, Z., Spooner, E., Li, E., Zhang, G., Colaiacovo, M., et al. (2006). Reversal of histone lysine trimethylation by the JMJD2 family of histone demethylases. Cell *125*, 467–481.

Xiao, T., Hall, H., Kizer, K.O., Shibata, Y., Hall, M.C., Borchers, C.H., and Strahl, B.D. (2003). Phosphorylation of RNA polymerase II CTD regulates H3 methylation in yeast. Genes Dev. *17*, 654–663.

Zhang, Y., Liu, T., Meyer, C.A., Eeckhoute, J., Johnson, D.S., Bernstein, B.E., Nusbaum, C., Myers, R.M., Brown, M., Li, W., and Liu, X.S. (2008). Model-based analysis of ChIP-seq (MACS). Genome Biol. *9*, R137.

STAR★METHODS

KEY RESOURCES TABLE

REAGENT or RESOURCE	SOURCE	IDENTIFIER
Antibodies		
Rabbit polyclonal anti-dKDM4A	modENCODE, this paper	Q2541
Mouse monoclonal anti-HP1a	Hybridoma Bank	Cat#C1A9; RRID: AB_528276
Mouse monoclonal anti-Tubulin	Sigma-Aldrich	Cat#T6199; RRID: AB_477583
Rabbit polyclonal anti-H3K36me3	Abcam	Cat#ab9050; RRID: AB_306966
Mouse monoclonal anti-H3K36me3	Wako	Cat#304-95282
Rabbit polyclonal anti-H3K9me3	Abcam	Cat#ab8898; RRID: AB_306848
Rabbit polyclonal anti-H3K9me2	ActiveMotif	Cat#39753
Rabbit polyclonal anti-γH2Av	VWR	Cat#600-401-914; RRID: AB_828383
Mouse monoclonal anti-γH2Av	Hybridoma Bank	Cat#UNC93-5.2.1; RRID: AB_2618077
Rabbit polyclonal anti-H2B	Millipore	Cat#07-371; RRID: AB_310561
Rabbit polyclonal anti-H3	Abcam	Cat#ab46765; RRID: AB_880439
Mouse monoclonal anti-Lamin	Hybridoma Bank	Cat#ADL67.10; RRID: AB_528336
Goat polyclonal anti-GFP	Rockland	Cat#RL600-101-215
Rabbit polyclonal anti-H3K56me3	Sandra B. Hake (Jack et al., 2013)	N/A
Chemicals, Peptides, and Recombinant Proteins		
DOTAP Liposomal Transfection Reagent	Roche	Cat#11202375001
TransIT-2020 Transfection Reagent	Mirus	Cat#MIR 5400
Critical Commercial Assays		
Quikchange Site-Directed Mutagenesis Kit	Agilent	Cat#200519
MEGAScript T7 Transcription kit	Life Technologies	Cat#AM1334
SuperSignal West Dura Chemiluminescence Kit	Pierce	Cat#34075
TruSeq RNA Sample Prep Kit	Illumina	Cat#RS-122-2001
TruSeq DNA Sample Prep Kit	Illumina	Cat#FC-121-1001
Deposited Data		
Raw and analyzed data	This paper	GEO: GSE99023
Raw and analyzed data	This paper	GEO: GSE99027
Experimental Models: Cell Lines		
D. melanogaster: Cell line S2	*Drosophila* Genomics Resource Center	Flybase: FBtc0000006
D. melanogaster: Cell line Kc	*Drosophila* Genomics Resource Center	Flybase: FBtc0000001
D. melanogaster: Cell line ML-DmBG3-c2	*Drosophila* Genomics Resource Center	Flybase: FBtc0000068
Experimental Models: Organisms/Strains		
D. melanogaster: KV135: KV135	Gary Karpen Laboratory, (Konev et al., 2003)	N/A
D. melanogaster: KV35: KV35	Gary Karpen Laboratory, (Konev et al., 2003)	N/A
D. melanogaster: KV169: KV169	Gary Karpen Laboratory, (Konev et al., 2003)	N/A
D. melanogaster: *dKDM4A*[*NP0618*]: w[*]; P{GawB}Kdm4A[NP0618] / CyO	Kyoto Stock Center	DGRC: 103678; Flybase: FBst0302546
D. melanogaster: *dKDM4A*[*KG04636*]: y[1] w[67c23]; P{y[+mDint2] w[BR.E.BR]= SUPor-P}Kdm4A[KG04636]	Bloomington *Drosophila* Stock Center	BDSC:13828; Flybase: FBst0013828
D. melanogaster: *mei-41*[*29D*]: *mei-41*[*29D*]	Tin Tin Su, (Laurencon et al., 2003)	Flybase: FBal0104998

(*Continued on next page*)

Continued

REAGENT or RESOURCE	SOURCE	IDENTIFIER
D. melanogaster: *mei-41*[*D3*]: *mei-41*[*D3*]	Tin Tin Su, (Sibon et al., 1999)	Flybase: FBal0012154
D. melanogaster: *mu2*[*1*]: mu2[1] st[1]/ TM6C, ca[1]	Bloomington *Drosophila* Stock Center	BDSC: 1220; Flybase: FBst0304923
D. melanogaster: *mus101*[*D1*]: w[1] mus101[D1]	Bloomington *Drosophila* Stock Center	BDSC:2310; Flybase: FBst0002310
D. melanogaster: *nbs1*[*1*]: nbs[1] kni[ri-1] p[p]/TM3, Sb[1]	Bloomington *Drosophila* Stock Center	BDSC:2554; Flybase: FBst0002554
D. melanogaster: *tefu*[*8*]: P{ry[+t7.2]=neoFRT}82B tefu[atm-8] e[1]/TM3, Sb[1]	Bloomington *Drosophila* Stock Center	BDSC:8624; Flybase: FBst0008624
D. melanogaster: *smc1*[*exc46*]: y[1] w[*]; SMC1[exc46]/TM3, Sb[1] Ser[1]	Scott Hawley, (Schuldiner et al., 2008)	Flybase: FBal0195335
D. melanogaster: *rod*[*EY04576*]: y[1] w [67c23]; P{w[+mC] y[+mDint2]=EPgy2}rod [EY04576]	Bloomington *Drosophila* Stock Center	BDSC:19842; Flybase: FBst0019842
D. melanogaster: *zw10*[*5*]: y[1] Zw10[5]/ FM7a/Dp(1;2;Y)w[+]	Bloomington *Drosophila* Stock Center	BDSC:4282; Flybase: FBst0004282
D. melanogaster: *Su*(*var*)*3-9*[*06*]: *Su*(*var*)*3-9*[*06*]	Gunter Reuter, (Tschiersch et al., 1994)	Flybase: FBal0016562
D. melanogaster: *Su*(*var*)*3-9*[*17*]: *Su*(*var*)*3-9*[*17*]	Gunter Reuter, (Tschiersch et al., 1994)	Flybase: FBal0039075
D. melanogaster: *pAct5C*::*GAL4*: y[1] w[*]; P{Act5C-GAL4-w}E1/CyO	Bloomington *Drosophila* Stock Center	BDSC:25374; Flybase: FBst0025374
D. melanogaster: *pUAS-dKDM4A*: Kdm4AScer\UAS.T:Ivir\ HA1,T:Zzzz\FLAG	Jerry Workman, (Lin et al., 2008)	Flybase: FBal0220513
D. melanogaster: *pUAS-V423A*: Kdm4AV423A.Scer\UAS.T:Ivir\ HA1,T:Zzzz\FLAG	Jerry Workman, (Lin et al., 2008)	Flybase: FBal0220514
D. melanogaster: *CaSper-dKDM4A*: Kdm4A[+tCa]	Mattias Mannervik, (Crona et al., 2013)	Flybase: FBal0284966
D. melanogaster: *CaSper-dKDM4A H195A*: dKDM4A[H195A]	Mattias Mannervik, (Crona et al., 2013)	Flybase: FBal0284967
D. melanogaster: *ΔdKDM4A*: ΔdKDM4A :	Mattias Mannervik, (Crona et al., 2013)	Flybase: FBal0284963
Oligonucleotides		
See Table S4.		
Recombinant DNA		
pCOPIA-GFP-dKDM4A	This paper	N/A
pCOPIA-GFP-dKDM4A-altcodon	This paper	N/A
pCOPIA-GFP-dKDM4A-H195A-altcodon	This paper	N/A
pCOPIA-mCherry-dKDM4A	This paper	N/A
pCOPIA-mCherry-dKDM4A-V423A	This paper	N/A
pCOPIA-GFP-HP1a	This paper	N/A
pCOPIA-mCherry-HP1a	This paper	N/A
pCOPIA-mCherry-PCNA	Barbara Mellone	N/A
pCOPIA-GFP-HOAP	This paper	N/A
pCoHygro	Life Technologies	N/A
Software and Algorithms		
SoftWoRx	Applied Precision, LLC	N/A
ImageJ/Fiji	(Schindelin et al., 2012)	https://imagej.net/Fiji
Bowtie	(Langmead et al., 2009)	http://bowtie-bio.sourceforge.net/index.shtml

(*Continued on next page*)

Continued

REAGENT or RESOURCE	SOURCE	IDENTIFIER
TopHat	(Trapnell et al., 2012)	http://ccb.jhu.edu/software/tophat/index.shtml
DESEQ2	(Love et al., 2014)	http://bioconductor.org/packages/release/bioc/html/DESeq2.html
Macs2	(Zhang et al., 2008)	https://pypi.python.org/pypi/MACS2/
Samtools	(Li et al., 2009)	http://samtools.sourceforge.net/

CONTACT FOR REAGENT AND RESOURCE SHARING

Further information and requests for resources and reagents should be directed to and will be fulfilled by the Lead Contact, Serafin U. Colmenares (sucolmenares@lbl.gov).

EXPERIMENTAL MODEL AND SUBJECT DETAILS

Schneider-2, Kc and BG3 cells were cultured at 25°C in standard medium with antibiotics and 10% FBS. Schneider-2 and BG3 cells are male, from late embryos and larval central nervous system, respectively; Kc cells are female from early embryos.

Drosophila strains were maintained on standard cornmeal/molasses/agar media at 22°C.

METHOD DETAILS

Plasmid Construction

HP1a and dKDM4A were cloned into pCOPIA vectors containing N-terminal GFP or mCherry epitope tags using Asc1 and Pac1 restriction sites (Chiolo et al., 2011). HOAP was similarly cloned into the pCOPIA-GFP vector. H195A and V423A dKDM4A mutations were generated using the Quikchange Site-Directed Mutagenesis kit (Agilent). dKDM4A containing C-terminal alternative codons was derived from a synthesized gene fragment (Genewiz) inserted into BsiWI and PacI restriction sites.

Fly Lines

Fly crosses were performed using standard genetic techniques. *dKDM4A*^{NP0618}, *pAct5C*::*GAL4* flies were generated by meiotic recombination and crossed as females. *Su*(*var*)*3-9* null flies, which are progeny of transheterozygotes of null alleles 6 and 17, and thereby lack both maternal and zygotic Su(var)3-9, were used in all experiments. KV fly lines containing SUPor-P inserted in various HC loci were previously generated (Konev et al., 2003). PEV assays were conducted on male KV flies, using a DFK41AF02 color camera (The Imaging Source), and analyzed using Fiji.

Tissue Culture Manipulation

Stable lines were generated by co-transfection of expression constructs with pCoHygro (Life Technologies) using the DOTAP Liposomal Transfection Reagent (Roche) and selection for hygromycin resistance at 100 ug/mL (Life Technologies). Transient transfections were conducted using the TransIT-2020 reagent (Mirus), and live imaging was performed 72 hours later. RNAi was performed with dsRNA generated from MEGAScript T7 Transcription kit (Life Technologies) and PCR products containing T7 promoter sequences and the target regions (Table S2). Tissue culture cells were treated with 5-10 ug of dsRNA for 5 days with DOTAP Reagent (Roche). Irradiation experiments were conducted by exposing cells to 5 Gy of X-rays from a 130 kv Faxitron TRX5200 and incubating them for various recovery times at 25°C. All results are based from at least two biological replicates.

Images were collected using an Applied Precision Deltavision microscope and analyzed using SoftworX software. FRAP experiments were conducted using a 488 nm QLM laser (Applied Precision) at 1 micron bleach size and 100% intensity, and images acquired using adaptive settings. Pre-bleach signal was set to 100% and used to normalize recovery signals.

FISH and Immunofluorescence

Tissue culture cells were fixed on slides with 3.6% paraformaldehyde for 5 minutes and permeabilized with 0.4% Triton-X in PBS. For time-course or parallel experiments, cells were fixed on chamber slides (Thermo Scientific) to ensure uniform treatment. Ovaries were dissected from 5-day old adult females and fixed whole-mount with 3.6% paraformaldehyde in PBS plus 0.4% Triton-X for 15 minutes. FISH was conducted by stepwise heating of samples from 37°C–70°C in 2X sodium citrate buffer with 0.1% Tween-20, followed by incubation with heat-denatured 2.5 ng/uL LNA or BNA probes (Integrated DNA Technologies) in 50% formamide, 2X sodium citrate buffer, 10% Dextran Sulfate for 3 hours at 37°C-50°C, depending on probe annealing temperature. Immunofluorescence was

performed in PBS+0.4% Triton-X with either 5% FBS or 1% milk blocking solutions and overnight incubations at 4°C with primary antibodies (1:1000 anti-HP1a, 1:1000 anti-γH2Av, 1:500 anti-H3K36me3, 1:500 anti-H3K9me2, 1:500 anti-GFP, 1:500 anti-H3K56me3) followed by 1 hour incubation at 25°C with secondary antibodies. Nuclei were counter-stained with DAPI and mounted in Prolong Gold Antifade (Life Technologies). All results are based from at least two biological replicates.

RNA-Seq and ChIP-Seq

Total RNA was harvested using Trizol reagent from 5 x 10^6 S2 cells, and mRNA was purified using oligo-dT-conjugated magnetic beads. Chromatin was prepared by fixation of 2x10^7 S2 cells with 1% paraformaldehyde for 10 minutes and shearing with Bioruptor sonicator (Diagenode). Immunoprecipitation was performed by overnight incubation of chromatin with Protein-A Dynabeads and 5 ug of either anti-H3K36me3 or anti-H3K9me3 ChIP-grade antibody (Abcam). Library construction from mRNA or immunoprecipitated DNA was conducted using TruSeq RNA and DNA sample preparation kits (Illumina). All sequencing data were obtained from the Vincent J. Coates Genomics Sequencing Laboratory at UC Berkeley.

Sequencing Analysis

Standard TopHat and DESeq2 programs were used to align and quantitate genic RNASeq data, and Bowtie was used to align ChIPSeq data, based on Release 5.2 assembly (Berkeley *Drosophila* Genome Project). Macs2 was used to perform normalization between input and ChIP sequences, and broadPeak calling was used to identify regions of enrichment. Peaks were grouped into EC or HC based on epigenomic borders of S2 cells (Riddle et al., 2011). Results are based from two biological replicates.

Western Blotting

Cell pellets flash frozen in liquid nitrogen were resuspended in Buffer A (50 mM Hepes pH 7.6, 10 mM KCl, 3 mM $MgCl_2$, 10% glycerol, 0.05% NP-40, 5 mM NaF, 5 mM β-glycerophosphate, 1 mM Benzamidine, 1X protease inhibitor cocktail (Roche), 1 mM PMSF). Cell extracts were treated with 10 units benzonase (Millipore) per 37 μg of chromatin (estimated by A_{260} reading) at 4°C with mixing for 30 min. and mixed with 5X SDS-PAGE loading buffer. Fly extracts were prepared similarly using a Dounce homogenizer. Standard SDS-PAGE and Western blot transfer protocols were used with nitrocellulose membranes and Tris-glycine buffer. Blots were probed with 1:1000 anti-dKDM4A, 1:1000 anti-HP1a, 1:2000 anti-H3, 1:2000 anti-H2B, 1:1000 anti-Lamin, 1:1000 anti-GFP, 1:2000 anti-tubulin, 1:500 anti-H3K56me3, 1:500 anti-H3K9me3, and 1:1000 anti-H3K36me3. Blots were imaged with SuperSignal West Dura chemiluminescence kit (Pierce) or Odyssey Imaging Systems (Li-cor), using appropriate secondary antibodies (Pierce, Li-cor).

QUANTIFICATION AND STATISTICAL ANALYSIS

Fly Viability

% viability (Table S3A) was calculated using the ratio of adult *dKDM4A* mutant heterozygotes (over balancer) to *dKDM4A* mutant homozygotes, normalized to the ratio of wild-type heterozygotes to homozygotes. Due to subviability of *dKDM4A* mutant flies, ratios obtained from double mutants of *dKDM4A* and another gene were normalized to ratios for the *dKDM4A* mutant alone, and adjusted to set the *dKDM4A* mutant at 100% to facilitate comparisons (Viability* in Tables 1 and S3). All genotypes analyzed were quantified from 5-15 crosses and conducted in a *y w* genetic background. Fertility was determined by testing if double mutants homozygous for *dKDM4A* mutation produced adult progeny.

ChIP-Seq and RNA-Seq

ChIP-seq peak enrichment values between RNAi treatments were analyzed using two-sample Kolmogorov-Smirnov test to calculate p-values and D-statistics. Counting of multicopy genes, transposable elements, and short repeats from either RNA-Seq or ChIP-Seq data was performed by alignment to a custom Bowtie index composed of 187 transposable elements, 11 tandem repeats, rDNA, and histone genes. Counts were normalized to the sum of reads aligned to the unique portion of the genome and reads aligned to the custom Bowtie index of repetitive DNA. Enrichment values of repetitive elements were then calculated by dividing the normalized counts of the treatment group by the control group in RNASeq, or by dividing normalized ChIP counts by input counts in ChIPSeq. Genes and repetitive elements from RNASeq data were simultaneously analyzed using DESEQ2 to identify significant changes ($p<0.05$) in transcriptional regulation between replicate experiments. For ChiPSeq, the standard deviation of mean enrichment values was used to conservatively identify repetitive DNAs that significantly changed in binding H3K36me3 or H3K9me3.

Western Blotting

To quantitate differences in protein levels during recovery from IR-induced DNA damage (Figure 6F), Fiji was used to measure Western blot band density from 4 independent experiments. Values were normalized to the mean of untreated GFP RNAi samples. SD was calculated, along with Wilcoxon rank test.

Image Analysis

Counting of γH2Av foci overlapping DAPI-bright or HP1a-rich domains and of FISH foci was conducted manually, N = 50-100 cells per timepoint/treatment. Results are based from at least two biological replicates. Standard error was calculated for repair kinetics, while p-values using the Student's t test, assuming two-sample tails and unequal variance, were calculated for both repair kinetics and FISH analysis.

DATA AND SOFTWARE AVAILABILITY

RNA-seq and ChIP-seq data are available using GEO accession numbers GSE99023 and GSE99027, respectively.